

Phenomenology of an E_6 inspired extension of Standard Model: Higgs sector

Sanchari Bhattacharyya* and Anindya Datta†

*Department of Physics, University of Calcutta
92, Acharya Prafulla Chandra Road, Kolkata 700009*

Abstract

We investigate a variant of Left-Right symmetric model based $SU(3)_C \otimes SU(2)_L \otimes U(1)_L \otimes SU(2)_R \otimes U(1)_R$ gauge group (32121). Spontaneous breaking of 32121 down to the Standard Model (SM) gauge group, requires a bi-doublet under $SU(2)_L \otimes SU(2)_R$, a right-handed doublet scalar under $SU(2)_R$ along with a $SU(2)$ singlet scalar boson. Symmetry breaking leads to several neutral and charged massive gauge bosons apart from the SM W and Z . The Large Hadron Collider (LHC) results for the search of heavy gauge bosons can be used to constrain the vacuum expectation values responsible for giving masses to these extra heavy gauge bosons. Physical spectrum of the scalar bosons contains several neutral CP-even and CP-odd states and a couple of charged scalars apart from the SM-like Higgs boson. We have put constraints on the masses of some of these scalars from the existing LHC data. The possible decay rates and production cross-sections of these scalars have been investigated in some details. Production cross-sections for some of the scalars look promising at 14 TeV and 27 TeV run of the LHC with high luminosity option. We keep, in our model, all the fermions present in the 27-dimensional fundamental representation of E_6 . Mass limit of one such exotic lepton has also been derived from present LHC data. It is noted that some of these neutral exotic lepton or neutral scalar bosons of this model can serve the purpose of a cold dark matter.

1 Introduction

The Standard Model (SM) of Particle Physics has been extremely successful in describing the interactions of elementary particles and fundamental forces operative in microscopic world. Probably, the most subtle prediction of the SM has been the existence of a scalar boson, the Higgs boson, responsible for giving masses to all the elementary particles. With the discovery of Higgs boson [1, 2] at the Large Hadron Collider (LHC), CERN; all the predictions of the SM has been tested. In spite of its immense success, SM in its original form, miserably fails to explain one important piece of experimental observations, namely, the existence of Dark Matter (DM), a new kind of very weakly interacting but massive matter pervading the whole universe. Moreover, it is very crucial to know whether the discovered 125 GeV Higgs boson is the sole agent for Electroweak Symmetry Breaking (EWSB) or a more rich scalar sector is responsible for such an act. There are several theoretical studies [3] which have been devoted to investigate the phenomenology of extended Higgs sectors. It is important to note that any model with extended scalar sector must contain a physical CP-even scalar boson with exactly the same properties of the SM Higgs. The extended scalar sector may also be instrumental in resolving some of the shortcomings of the SM. As for example, extended Higgs sectors with singlet scalars may resolve the problem of dark matter [4]. Left-Right (LR) symmetric triplet Higgs models are very popular in explaining neutrino masses via seesaw mechanisms [5], [6]. Multi-Higgs doublet models have been used in explaining flavour problems [7]. An added bonus for many such

*sanchari1192@gmail.com

†adphys@caluniv.ac.in

models with extended Higgs sector is possibility of a stable neutral scalar which may act as a suitable candidate for DM. On the experimental front, signatures for extra neutral and charged scalar bosons have already been in the top of the agenda for all the past and present experimental programmes. Unfortunately, the evidence for the SM-like Higgs boson has been observed so far. Present precision of experimental data on Higgs signal strengths in different channels and our lack of experimental knowledge on Higgs tri-linear coupling limit us from conclusively decide whether the 125 GeV boson is the only agent of EWSB [8]. In near future, with high luminosity (HL) 14 (27) TeV run of the LHC we expect these pictures to be more clearer. So it is of utmost priority for particle physics community to construct such models with extended scalar and/or gauge sector and check whether these models are consistent with the available and future experimental data from the LHC. A number of such models have been proposed and their possible experimental signatures at the LHC have been sought for. Unfortunately, many such efforts have been futile so far. Non-observation of any signature of Physics beyond the SM (whether supersymmetry [9] or extra-dimension [10]), only pushes the scale of such new dynamics in upward direction.

In an endeavour to construct a model which has a rich scalar sector satisfying the LHC data we turn our attention to an unifying gauge group E_6 [11], which can be broken down to $[SU(3)]^3$ followed by a further breakdown to $SU(3)_C \otimes SU(2)_L \otimes U(1)_L \otimes SU(2)_R \otimes U(1)_R$ (32121). We will not be interested in the dynamics which may be responsible for the aforementioned symmetry breaking chain, rather we will be investigating the appearance of SM gauge group from 32121 and the resulting phenomenology of additional particles and their interactions among themselves or with the particles of SM. The main advantage of working in a framework of unifying group like E_6 is the natural appearance of right-handed neutrinos as well as 3 generations of heavy neutral leptons, singlet under either of $SU(2)$ groups. The right-handed heavy neutrinos may be responsible for neutrino mass generations via the (Type-I) seesaw mechanism. This model contains a large number of neutral and charged scalar bosons after the spontaneous breakdown of $SU(2)_L \otimes U(1)_L \otimes SU(2)_R \otimes U(1)_R$ to EW gauge group of the SM. These color singlet scalars originate from $(\mathbf{1}, \mathbf{3}, \bar{\mathbf{3}})$ representation of $[SU(3)]^3$. The presence of such rich scalar sector is one of the reasons behind the present investigation. Furthermore, several exotic fermions will arise from the 27-dimensional fundamental representation of E_6 . Some of the neutral Higgs bosons and charge neutral leptons may also serve the purpose of dark matter. However, in this article we will mainly investigate the phenomenology of the extended scalar sector. A separate study will be devoted to the DM aspect of this model.

Although, the scalar sector of the model under consideration have many similarities with that of the left-right model (LRM), the phenomenology of the scalar sector has some distinct features which are different from left-right symmetric model (LRSM). In the present work, we have banked on these features of the model to distinguish it from the often studied models like LRSM. Let us emphasise on the novelty of the present work in the following.

- Although the 32121 gauge group respects the LR symmetry, the model under consideration is different from the conventional LRS model. The first hint of this difference comes from the fact that both the bi-doublet vacuum expectation values (vevs) k_1 and k_2 cannot be simultaneously set to non-zero values unlike its more familiar variant based on $SU(2)_L \times SU(2)_R \times U(1)_{B-L}$ unless we consider a tri-linear term in the scalar potential. Even after adding such a term which comes out to be small along with small value of k_2 , phenomenology of this model remains practically the same as $k_2 = 0$ case. This makes the phenomenology of the scalar sector of 32121 model different from LRSM.
- We have considered the complete set of fermions arising from the **27**-dimensional representation of E_6 . Some of these fermions are stable but have electric charges. We have for the first time derived bounds on their masses from the present LHC data. A detailed endeavour from the experimentalist friends to study their signature including detector simulation is presently unavailable and is urgently needed.
- Although one of the charged Higgs bosons arising in the model has conventional decay to tb , the other one is stable and produces a charged track in the detector. Such stable charged bosons are not present in the LRSM and their signatures have not been discussed in the present literature so far.
- The pair-production of charged and neutral Higgs bosons arising from left-handed doublet will produce either two charged tracks or a single charged track in the detector, giving rise to a background free novel signature of this model.
- Presence of a heavy neutral gauge boson, A' apart from Z' (arising because of the presence of $SU(2)_R$, can be identified with the Z_R in LRSM) is also a hall mark of the model under the consideration. This neutral boson arises due to the extra $U(1)$ factor in 32121 and couples to all the SM fermions, in contrast to several extensions of the SM by an extra $U(1)$, where this heavy neutral state have selective coupling with the SM

fermions. Unlike the LRS model, where only one heavy neutral gauge boson is present, 32121 is characterised by two such states with similar properties but having different masses.

- Three possible Dark Matter candidates in forms of exotic fermion, a scalar and a pseudoscalar originating from left-doublet, are present in the spectrum. Although we will not discuss the direct detection bounds or relic density, an lower bound on the mass of the scalar has been derived indirectly from the LHC data in the present analysis.

Before we come to an end of this section, it is important to mention that we have only guided by the framework of E_6 to study the phenomenology of the a set of scalars whose masses are somehow interlaced due to the structure of the scalar potential respecting the local 32121 gauge symmetry. Similarly, the gauge group and complete set of 27-plet of of fermions are chosen from a low energy point of view. Let us re-emphasize that we will not study the symmetry breaking chain $E_6 \rightarrow [SU(3)]^3 \rightarrow 32121$, neither we start with an unifying Yukawa texture appropriate for E_6 starting from GUT scale to generate the same at EW scale by renormalization group equation (RGE) running. The Yukawa matrices in our analysis, have been assumed to be non-diagonal. However, we will not discuss the pattern of masses and mixings for the exotic fermions present in the spectrum. The physical masses and mixings (in case of SM sector) have been assumed to be in consistence with the observed values of SM fermions while, for the exotic sector, they are free parameters defined at the EW scale. So, our connection to E_6 is only confined to the choice of gauge group and choice of fermions at low energy, without considering any effect from high scale physics creeping in due to renormalization.

Plan of the article is the following. In Section 2, we discuss the symmetry breaking mechanism and spectra of Higgs bosons after Spontaneous Symmetry Breaking (SSB). This section will also contain a discussion of gauge boson masses and fermion Yukawa interaction with the scalars. In the next section we will discuss in detail the phenomenology of the physical Higgs bosons which arise in the model after SSB. The decay branching ratios (BR) and production cross-sections of such Higgs bosons are presented in Section 3 in the context of 14 and 27 TeV run of the LHC. Finally, we conclude in Section 4 .

2 The description of $SU(3)_C \otimes SU(2)_L \otimes U(1)_L \otimes SU(2)_R \otimes U(1)_R$ model

In this article, we will be interested in an extension of the SM whose root can be traced back to the Grand Unified Group E_6 . However at the energy scale of LHC experiment in which we are interested, we keep all the fermions and Higgs multiplets excepting few colored scalar bosons, which naturally arise in the 27-dimensional fundamental representation of E_6 . However, to keep the number of matter fields in our model to a minimum, we will assume that the colored scalars are too heavy (of the order of symmetry breaking scale of $[SU(3)]^3$) to affect the phenomenology at the LHC energy¹. Higgs multiplets will be instrumental in breaking down $SU(3)_C \otimes SU(2)_L \otimes U(1)_L \otimes SU(2)_R \otimes U(1)_R$ to the SM the gauge group. While the complete set of fermions present in 27-plet are necessary for anomaly cancellation. However, this choice of fermion representations used in our analysis is no way unique. One can have vanishing anomaly contribution only by considering the left and right-handed fermion doublets L_L , L_R , Q_L and Q_R . Hyper-charge assignments of the rest of the fermion multiplets listed in Table 1 can then be done by the consideration of anomaly cancellation among the exotic fermions and can be done in more than one ways. We have presented two such cases in the Table 2. It is important to note that in such a situation, $U(1)_{L,R}$ charges for the Higgs multiplets will be different from the case presented in this analysis. However, we will not consider such a situation and present our phenomenological analysis with complete set of fermions arising from the 27-plet.

Gauge bosons present in this model automatically follows from the gauge group of our interest. The matter and gauge fields which are present in our model are listed in Table 1².

The first block represents the minimal matter contents in the fermion sector, i.e., SM-fermions with right-handed neutrino. The scalars in the next block will provide us a gauge invariant Yukawa Lagrangian generating the masses of the SM-fermions and Majorana mass for ν_R . We can generate the masses of all the exotic fermions with Φ_S .

¹If we intend to break the $[SU(3)]^3$ to 31221 by embedding the former into a 5-dimensional manifold and applying appropriate orbifold boundary conditions, one may get rid of such colored scalars by choosing appropriate boundary conditions on these fields at the orbifold boundaries. [12]

²Electric charge, Q is defined through the relation, $Q = T_{3L} + T_{3R} + Y_L/2 + Y_R/2$. L and R carry their usual meaning. These quantum numbers for each multiplet of 32121 model have been noted in the Table 1

		3_C	2_L	2_R	1_L	1_R
Fermions	L_L	1	2	1	-1/6	-1/3
	\bar{L}_R	1	1	2	1/3	1/6
	\bar{L}_B	1	2	2	-1/6	1/6
	\bar{L}_S	1	1	1	1/3	-1/3
	Q_L	3	2	1	1/6	0
	\bar{Q}_R	$\bar{3}$	1	2	0	-1/6
	\bar{Q}_{LS}	$\bar{3}$	1	1	-1/3	0
	Q_{RS}	3	1	1	0	1/3
Bosons	Φ_B	1	2	2	1/6	-1/6
	Φ_L	1	2	1	1/6	1/3
	Φ_R	1	1	2	-1/3	-1/6
	Φ_S	1	1	1	-1/3	1/3
Gauge bosons	$G^i, i = 1, \dots, 8$	8	1	1	0	0
	$W_L^i, i = 1, 2, 3$	1	3	1	0	0
	$W_R^i, i = 1, 2, 3$	1	1	3	0	0
	B_L	1	1	1	0	0
	B_R	1	1	1	0	0

Table 1: Fermions and Bosons in 32121 model with their respective quantum numbers

	3_C	2_L	2_R	1_L	1_R
L_L	1	2	1	1	-3/2
\bar{L}_R	1	1	2	-1	3/2
Q_L	3	2	1	-1/3	1/2
\bar{Q}_R	$\bar{3}$	1	2	1/3	-1/2
Φ_B	1	2	2	0	0
Φ_R	1	1	2	1	-3/2
Φ_S	1	1	1	0	0
\bar{L}_B	1	2	2	0	0
\bar{Q}_{LS}	$\bar{3}$	1	1	1/3	1/3
Q_{RS}	3	1	1	-1/3	-1/3
\bar{L}_S	1	1	1	0	0

Table 2: Fermions and Scalars in 32121 model with their respective quantum numbers. The important thing to note here that, the $U(1)_L$ hypercharges of Q_{LS} and Q_{RS} have to be same to cancel chiral anomaly. Similar for the case of $U(1)_R$ too. But $U(1)_L$ and $U(1)_R$ hypercharges for each of them may not be equal. That depends upon the charge assignment of Q_{LS}, Q_{RS} . However, we consider Q_{LS}, Q_{RS} have 2/3 charge. So it is an easy way to choose the $U(1)_L$ and $U(1)_R$ hypercharges of Q_{LS} as well as Q_{RS} to be equal i.e., 1/3.

The third block represents the other beyond Standard Model (BSM) fermions present in **27**-plet and separately cancels chiral anomaly. L_B is SU(2) doublet but U(1) singlet, L_S is pure singlet. Here are two cases. For Q_{LS} as well as Q_{RS} separately,

(i) If $U(1)_L$ hypercharge is equal to $U(1)_R$ hypercharge (i.e., same value/sign), Q_{LS}, Q_{RS} will be vector-like

and they will not contribute in anomaly cancellation.

(ii) If $U(1)_L$ hypercharge is not equal to $U(1)_R$ hypercharge (i.e., different value/sign), Q_{LS}, Q_{RS} will be chiral fermions and will contribute in anomaly cancellation.

2.1 Scalar sector of $SU(3)_C \otimes SU(2)_L \otimes U(1)_L \otimes SU(2)_R \otimes U(1)_R$ model

We now briefly discuss the Higgs multiplets responsible for symmetry breaking and their interactions in this model. The scalar sector of the 32121 model contains one Higgs bi-doublet (Φ_B), one left-handed (Φ_L), one right-handed (Φ_R) weak doublets and a singlet Higgs boson (Φ_S) with non-zero $U(1)$ charges. These scalars arise from the $(\mathbf{1}, \mathbf{3}, \mathbf{\bar{3}})$ representation of $[SU(3)]^3$. For a complete symmetry breaking mechanism from $32121 \rightarrow SU(3)_C \otimes SU(2)_L \otimes U(1)_Y \rightarrow SU(3)_C \otimes U(1)_{EM}$, the alignments of Higgs bi-doublet, right (left)-handed doublet and the singlet will be the following.

$$\begin{aligned}\Phi_B &= \begin{pmatrix} \frac{1}{\sqrt{2}}(k_1 + h_1^0 + i\xi_1^0) & h_1^+ \\ h_2^- & \frac{1}{\sqrt{2}}(k_2 + h_2^0 + i\xi_2^0) \end{pmatrix}, \\ \Phi_L &= \begin{pmatrix} h_L^+ \\ \frac{1}{\sqrt{2}}(v_L + h_L^0 + i\xi_L^0) \end{pmatrix}, \Phi_R = \begin{pmatrix} \frac{1}{\sqrt{2}}(v_R + h_R^0 + i\xi_R^0) \\ h_R^- \end{pmatrix}, \Phi_S = \frac{1}{\sqrt{2}}(v_S + h_S^0 + i\xi_S^0)\end{aligned}\quad (1)$$

The Higgs potential, \mathcal{V} which obeys symmetry of the gauge group can be written as sum of two parts \mathcal{V}_1 and \mathcal{V}_2 , where,

$$\begin{aligned}\mathcal{V}_1 &= -\mu_1^2 Tr(\Phi_B^\dagger \Phi_B) - \mu_3^2 (\Phi_L^\dagger \Phi_L + \Phi_R^\dagger \Phi_R) - \mu_4^2 \Phi_S^\dagger \Phi_S \\ &+ \lambda_1 Tr[(\Phi_B^\dagger \Phi_B)^2] + \lambda_3 (Tr[\Phi_B^\dagger \tilde{\Phi}_B] Tr[\tilde{\Phi}_B^\dagger \Phi_B]) \\ &+ \alpha_1 (\Phi_S^\dagger \Phi_S)^2 + \beta_1 Tr[\Phi_B^\dagger \Phi_B] (\Phi_S^\dagger \Phi_S) + \gamma_1 [(\Phi_L^\dagger \Phi_L) + (\Phi_R^\dagger \Phi_R)] (\Phi_S^\dagger \Phi_S) \\ &+ \rho_1 [(\Phi_L^\dagger \Phi_L)^2 + (\Phi_R^\dagger \Phi_R)^2] + \rho_3 [(\Phi_L^\dagger \Phi_L)(\Phi_R^\dagger \Phi_R)] + c_1 Tr[\Phi_B^\dagger \Phi_B] [(\Phi_L^\dagger \Phi_L) + (\Phi_R^\dagger \Phi_R)] \\ &+ c_3 [(\Phi_L^\dagger \Phi_B \Phi_B^\dagger \Phi_L) + (\Phi_R^\dagger \Phi_B \Phi_B^\dagger \Phi_R)] + c_4 [(\Phi_L^\dagger \tilde{\Phi}_B \tilde{\Phi}_B^\dagger \Phi_L) + (\Phi_R^\dagger \tilde{\Phi}_B \tilde{\Phi}_B^\dagger \Phi_R)]\end{aligned}\quad (2)$$

and,

$$\mathcal{V}_2 = \mu_{BS} Tr[\Phi_B^\dagger \tilde{\Phi}_B] \Phi_S^* + h.c. \quad (3)$$

All the parameters in \mathcal{V} are considered to be real excluding any possibility of CP-violation via the Higgs sector. \mathcal{V} has a symmetry under $L \leftrightarrow R$ exchange. In the above, $\tilde{\Phi}_B \equiv \sigma_2 \Phi_B^* \sigma_2$.

We note that \mathcal{V}_1 has a symmetry corresponding to global phase transformations on the fields

$$\Phi_B \rightarrow e^{i\theta_B} \Phi_B; \quad \Phi_L \rightarrow e^{i\theta_L} \Phi_L; \quad \Phi_R \rightarrow e^{i\theta_R} \Phi_R \text{ and } \Phi_S \rightarrow e^{i\theta_S} \Phi_S. \quad (4)$$

However, \mathcal{V}_2 which is proportional to μ_{BS} , breaks this global symmetry explicitly (for example see ref. [13]) otherwise respecting the symmetries of 32121 gauge group. This results into appearance of bilinear terms like $h_1^0 h_2^0, h_1^+ h_2^-$. However, with both $k_1, k_2 \neq 0$ such bilinear terms also could be generated from the term proportional to λ_3 . Setting one of these vevs to zero automatically prohibits the appearance of such bilinear terms in the scalar potential. In other words, setting both k_1 and k_2 to their non-zero values excluding \mathcal{V}_2 , would break the global symmetry in Eq. 4 spontaneously which results into undesirable extra massless scalar modes. One can of course have non-zero k_1 and k_2 simultaneously, however in such a case, a tri-linear term proportional to μ_{BS} is necessary to break the global symmetry explicitly and thus avoiding the appearance of extra Goldstone modes.

The kinetic Lagrangian for scalars is,

$$\mathcal{L}_\Phi = Tr[(\mathcal{D}_\mu \Phi_B)^\dagger (\mathcal{D}^\mu \Phi_B)] + (\mathcal{D}_\mu \Phi_L)^\dagger (\mathcal{D}^\mu \Phi_L) + (\mathcal{D}_\mu \Phi_R)^\dagger (\mathcal{D}^\mu \Phi_R) + (\mathcal{D}_\mu \Phi_S)^\dagger (\mathcal{D}^\mu \Phi_S) \quad (5)$$

It is needless to mention that covariant derivatives acting on different Higgs multiplets, are not same and contain appropriate gauge bosons in them.

Minimization conditions we obtain are the following,

$$2\sqrt{2}\mu_{BS}k_2v_S + k_1(2\lambda_1k_1^2 + 2(\lambda_1 + 2\lambda_3)k_2^2 - 2\mu_1^2 + (c_1 + c_4)v_L^2 + (c_1 + c_3)v_R^2 + \beta_1v_S^2) = 0 \quad (6)$$

$$2\sqrt{2}\mu_{BS}k_1v_S + k_2(2\lambda_1k_2^2 + 2(\lambda_1 + 2\lambda_3)k_1^2 - 2\mu_1^2 + (c_1 + c_3)v_L^2 + (c_1 + c_4)v_R^2 + \beta_1v_S^2) = 0 \quad (7)$$

$$v_L [(c_1 + c_4)k_1^2 + (c_1 + c_3)k_2^2 - 2\mu_3^2 + 2\rho_1v_L^2 + \rho_3v_R^2 + \gamma_1v_S^2] = 0 \quad (8)$$

$$v_R [(c_1 + c_3)k_1^2 + (c_1 + c_4)k_2^2 - 2\mu_3^2 + 2\rho_1v_R^2 + \rho_3v_L^2 + \gamma_1v_S^2] = 0 \quad (9)$$

$$2\sqrt{2}k_1k_2\mu_{BS} + v_S(\beta_1(k_1^2 + k_2^2) - 2\mu_4^2 + \gamma_1(v_L^2 + v_R^2) + 2\alpha_1v_S^2) = 0 \quad (10)$$

From Eqs. 6 and 7,

$$\mu_1^2 = \frac{1}{2k_1} \left(2\sqrt{2}\mu_{BS}k_2v_S + k_1(2k_1^2\lambda_1 + 2(\lambda_1 + 2\lambda_3)k_2^2 + (c_1 + c_4)v_L^2 + (c_1 + c_3)v_R^2 + \beta_1v_S^2) \right) \quad (11)$$

$$\mu_1^2 = \frac{1}{2k_2} \left(2\sqrt{2}\mu_{BS}k_1v_S + k_2(2k_2^2\lambda_1 + 2(\lambda_1 + 2\lambda_3)k_1^2 + (c_1 + c_3)v_L^2 + (c_1 + c_4)v_R^2 + \beta_1v_S^2) \right) \quad (12)$$

Using Eqs. 11 and 12 for $k_1, k_2 \neq 0$, we have,

$$\mu_{BS} = \frac{1}{\sqrt{2}v_S} \frac{k_1k_2}{k_2^2 - k_1^2} \left((c_3 - c_4) \frac{v_L^2 - v_R^2}{2} - 2\lambda_3(k_2^2 - k_1^2) \right) \quad (13)$$

Spontaneous breaking of Left-Right symmetry demands, $v_R \neq 0$. Thus Eq. (9) results into,

$$\mu_3^2 = \frac{1}{2} [(c_1 + c_3)k_1^2 + \rho_3v_L^2 + 2\rho_1v_R^2 + \gamma_1v_S^2]. \quad (14)$$

The choice $v_L \neq 0$ leads to appearance of an extra massless scalar mode which is undesirable³ scalar potential. So we stick to the case with $v_L = 0$.

To break the extra $U(1)$ we have to opt for $v_S \neq 0$ resulting into (from Eq. 10),

$$\mu_4^2 = \frac{1}{2v_S} \left(2\sqrt{2}k_1k_2\mu_{BS} + v_S(\beta_1(k_1^2 + k_2^2) + \gamma_1(v_L^2 + v_R^2) + 2\alpha_1v_S^2) \right) \quad (15)$$

Once we fix the minimisation conditions of the Higgs potential, we are ready to note the Higgs mass matrices under such alignment of vacuum. However before delving into the details of scalar mass matrices let us make some brief comments on an important issue related to the minimum of the scalar potential. It is important to note that a scalar potential such as Eq. 2 depending on so many fields may have more than one minima having varying depths. Thus merely satisfying the minimisation condition (by scalar potential parameters) does not ascertain that one is at the deepest minimum of the potential. In principle, different choices of the scalar potential parameters correspond to minima of different depths. Moreover, radiative corrections can significantly change to the structure of scalar potential and consequently change the depths of different minima of the potential. Hence, it is expected that one must at least incorporate one-loop corrections to the scalar potential to before looking for the deepest minima. However the exercise of calculating an effective potential at one loop for our model is beyond the scope of the present analysis. So we stick to the tree level potential and have not tried to look for its deepest minima. As long as the tunnelling time from the false vacuum to the true (deepest) vacuum is larger than the lifetime of the Universe, sitting at a minimum other than the deepest one is not always hazardous. However a realistic estimation of this tunnelling time also requires a one loop corrected effective potential of our model. A recent study [14] has been devoted to the analysis of the tree level scalar potential with particular emphasis on vacuum alignment and structure of minima of the potential. We would like to note that alignment of the vacuum used in our analysis satisfies the criterion of a *good vacuum* ala [14].

In the following, we note the CP-even, CP-odd and charged scalar mass matrices after replacing μ_1 , μ_{BS} , μ_3 and μ_4 using Eqs. 11, 13, 14 and 15 respectively.

³This is related to the spontaneous breakdown of a global symmetry of the defined in Eq. 4.

In a basis, defined by the fields $\{h_1^0, h_2^0, h_L^0, h_R^0, h_S^0\}$ the square of CP-even mass matrix (M_r^{02}) is,

$$\begin{pmatrix} 2\lambda_1 k_1^2 + k_2^2 \Delta' & 2\lambda_1 k_1 k_2 + k_1 k_2 \Delta' & 0 & (c_1 + c_3)k_1 v_R & \beta_1 k_1 v_S - \frac{k_1 k_2^2 \Delta'}{v_S} \\ 2\lambda_1 k_1 k_2 + k_1 k_2 \Delta' & 2\lambda_1 k_2^2 + k_1^2 \Delta' & 0 & (c_1 + c_4)k_2 v_R & \beta_1 k_2 v_S - \frac{k_1^2 k_2 \Delta'}{v_S} \\ 0 & 0 & \frac{1}{2}[(c_4 - c_3)k_-^2 + (\rho_3 - 2\rho_1)v_R^2] & 0 & 0 \\ (c_1 + c_3)k_1 v_R & (c_1 + c_4)k_2 v_R & 0 & 2\rho_1 v_R^2 & \gamma_1 v_R v_S \\ \beta_1 k_1 v_S - \frac{k_1 k_2^2 \Delta'}{v_S} & \beta_1 k_2 v_S - \frac{k_1^2 k_2 \Delta'}{v_S} & 0 & \gamma_1 v_R v_S & 2\alpha_1 v_S^2 + \frac{k_1^2 k_2^2 \Delta'}{v_S^2} \end{pmatrix} \quad (16)$$

where, $k_{\pm}^2 = k_1^2 \pm k_2^2$ and $\Delta' = \frac{(4\lambda_3 k_-^2 + (c_4 - c_3)v_R^2)}{2k_-^2}$.

While, the square of CP-odd mass matrix (M_i^{02}) in $\{\xi_1^0, \xi_2^0, \xi_L^0, \xi_R^0, \xi_S^0\}$ basis is,

$$\begin{pmatrix} k_2^2 \Delta' & k_1 k_2 \Delta' & 0 & 0 & \frac{k_1 k_2^2 \Delta'}{v_S} \\ k_1 k_2 \Delta' & k_1^2 \Delta' & 0 & 0 & \frac{k_1^2 k_2 \Delta'}{v_S} \\ 0 & 0 & \frac{1}{2}[(c_4 - c_3)(k_1^2 - k_2^2) + (\rho_3 - 2\rho_1)v_R^2] & 0 & 0 \\ 0 & 0 & 0 & 0 & 0 \\ \frac{k_1 k_2^2 \Delta'}{v_S} & \frac{k_1^2 k_2 \Delta'}{v_S} & 0 & 0 & \frac{k_1^2 k_2^2 \Delta'}{v_S^2} \end{pmatrix} \quad (17)$$

Once we diagonalise the above matrix, the three zero eigenvalues of CP-odd mass matrix corresponds to three Goldstone bosons responsible for giving masses to heavy neutral gauge bosons.

Square of the charged scalar mass matrix ($M^{\pm 2}$), in the basis $\{h_1^+, h_2^+, h_L^+, h_R^+\}$ is the following,

$$\begin{pmatrix} \frac{(c_4 - c_3)k_1^2 v_R^2}{2k_-^2} & \frac{(c_4 - c_3)k_1 k_2 v_R^2}{2k_-^2} & 0 & \frac{1}{2}(c_3 - c_4)k_1 v_R \\ \frac{(c_4 - c_3)k_1 k_2 v_R^2}{2k_-^2} & \frac{(c_4 - c_3)k_2^2 v_R^2}{2k_-^2} & 0 & \frac{1}{2}(c_3 - c_4)k_2 v_R \\ 0 & 0 & \frac{1}{2}(\rho_3 - 2\rho_1)v_R^2 & 0 \\ \frac{1}{2}(c_3 - c_4)k_1 v_R & \frac{1}{2}(c_3 - c_4)k_2 v_R & 0 & \frac{1}{2}(c_4 - c_3)k_-^2 \end{pmatrix} \quad (18)$$

Diagonalisation of the above matrix gives us two massive charged scalars and two massless Goldstones corresponding to a couple of heavy charged gauge bosons.

We note that, with non-zero k_1 and k_2 , W (and Z)-masses get contribution proportional to $(k_1^2 + k_2^2)^{\frac{1}{2}}$ while $W_L - W_R$ mixing is proportional to $\frac{k_1 k_2}{v_R^2}$ (see Eq. 27). Experimental limit on the $W_L - W_R$ mixing [15] forces one to choose *any one* of these vevs to be very small⁴ compared to other keeping $(k_1^2 + k_2^2)^{\frac{1}{2}}$ fixed at 246 GeV. One can then safely assume $k_1^2 + k_2^2 \approx k_1^2 - k_2^2 \approx k_1^2$.

Thus in small k_2 limit, we can rewrite the scalar mass matrices as,

$$M_r^{02} = \begin{pmatrix} 2\lambda_1 k_1^2 & 0 & 0 & (c_1 + c_3)k_1 v_R & \beta_1 k_1 v_S \\ 0 & \frac{1}{2}[4\lambda_3 k_1^2 + (c_4 - c_3)v_R^2] & 0 & 0 & 0 \\ 0 & 0 & \frac{1}{2}[(c_4 - c_3)k_1^2 + (\rho_3 - 2\rho_1)v_R^2] & 0 & 0 \\ (c_1 + c_3)k_1 v_R & 0 & 0 & 2\rho_1 v_R^2 & \gamma_1 v_R v_S \\ \beta_1 k_1 v_S & 0 & 0 & \gamma_1 v_R v_S & 2\alpha_1 v_S^2 \end{pmatrix} \quad (19)$$

$$M_i^{02} = \begin{pmatrix} 0 & 0 & 0 & 0 & 0 \\ 0 & \frac{1}{2}[4\lambda_3 k_1^2 + (c_4 - c_3)v_R^2] & 0 & 0 & 0 \\ 0 & 0 & \frac{1}{2}[(c_4 - c_3)k_1^2 + (\rho_3 - 2\rho_1)v_R^2] & 0 & 0 \\ 0 & 0 & 0 & 0 & 0 \\ 0 & 0 & 0 & 0 & 0 \end{pmatrix} \quad (20)$$

⁴e.g. If we set the mixing angle of $W_L - W_R$ at its maximum allowed value, k_2 will be of the order of 0.27 GeV, assuming $k_1 > k_2$.

$$M^{\pm 2} = \begin{pmatrix} \frac{1}{2}(c_4 - c_3)v_R^2 & 0 & 0 & \frac{1}{2}(c_3 - c_4)k_1v_R \\ 0 & 0 & 0 & 0 \\ 0 & 0 & \frac{1}{2}(\rho_3 - 2\rho_1)v_R^2 & 0 \\ \frac{1}{2}(c_3 - c_4)k_1v_R & 0 & 0 & \frac{1}{2}(c_4 - c_3)k_1^2 \end{pmatrix} \quad (21)$$

It is also evident that inspite of setting $k_2 = 0$ and as a consequence $\mu_{BS} = 0$, the elements of scalar mass matrices, mass eigenvalues and mixing matrices practically remains the same as before. It is easy to verify that in the limit $v_R, v_S \gg k_1 \gg k_2$ (the first inequality arises from the experimental lower limits on heavy gauge boson masses, discussed in a following section), mass matrix defined in Eq. 16 will practically produce the same eigenvalues and mixing among the scalars as has been resulted from Eq. 19. Similarly Eqs. 17 and 18 will generate same masses and mixings as Eqs. 20 and 21 will do respectively.

As mentioned above, the masses and mixings among the scalars in $k_2 \neq 0$, $\mu_{BS} \neq 0$ case are nearly same as the $k_2 = 0$ case, Although, a non-zero k_2 would result into some new couplings among the scalars which are not present in the later case. Some new decay channels will open up for the scalars like h_2^0 and H_S^0 . However, these new decay modes will not affect the decay patterns of the physical scalars in a significant way as the decay rates will be proportional to k_2^2 . We will not discuss them any further. All the following analysis will be done in $k_2 = 0$ limit which could be viewed as some special but not phenomenologically different from the more general situation with both k_1 and k_2 set to non-zero values.

The scalar potential has 10 real parameters, $\lambda_1, \lambda_3, \rho_1, \rho_3, c_1, c_3, c_4, \alpha_1, \beta_1$ and γ_1 . In order to find a set of acceptable values of the physical Higgs boson masses and the potential to be stable at least at classical level, the parameters of scalar potential must obey the following conditions.

$$\lambda_1, (\lambda_1 + 2\lambda_3), \rho_1, \rho_3, (c_1 + c_3), (c_1 + c_4), \alpha_1, \beta_1, \gamma_1 > 0 \quad (22)$$

The condition that the physical charged Higgs mass squares be positive, demands

$$c_4 - c_3 > 0 \text{ and } \rho_3 - 2\rho_1 > 0$$

Values of $(c_4 - c_3)$ and $(\rho_3 - 2\rho_1)$ can be constrained from a model independent experimental limit of charged Higgs boson mass.

From the CP-even scalar mass matrix we notice that it is effectively a 3×3 mass matrix in $\{h_1^0, h_R^0, h_S^0\}$ basis and thus difficult to diagonalise analytically. However, one linear combination of h_1^0, h_R^0 and h_S^0 will be definitely like the SM Higgs boson with mass 125 GeV and having similar properties with this.

$$M_{r3 \times 3}^{02} = \begin{pmatrix} 2\lambda_1 k_1^2 & (c_1 + c_3)k_1v_R & \beta_1 k_1v_S \\ (c_1 + c_3)k_1v_R & 2\rho_1 v_R^2 & \gamma_1 v_R v_S \\ \beta_1 k_1v_S & \gamma_1 v_R v_S & 2\alpha_1 v_S^2 \end{pmatrix} \quad (23)$$

We will denote the eigenstates of mass matrix (Eq. 23) by h^0, H_R^0, H_S^0 . The rest of the two massive CP-even and two massive CP-odd scalars do not mix with others, and we shall use the same notation to identify the mass eigenstates as we have used to define gauge eigenstates. For the charged Higgs sector, the two massive eigenstates will be denoted by H_L^\pm (which is a linear combinations of h_1^\pm and h_R^\pm) and H_L^\pm .

The 3×3 block of neutral CP-even mass matrix (see mass matrix (23)), can be diagonalised numerically. We must keep in mind that one of the eigenstates must correspond to the SM-like Higgs boson h^0 . This implies that the mass eigenvalue and the corresponding eigenvector must be consistent with the measured value of SM Higgs boson mass and its signal strengths to different decay channels at the LHC. We have done a scan over the parameters of the mass matrix (Eq. 23) over a range keeping the values of k_1, v_R and v_S fixed. We will see in the next section that the value of k_1 is fixed from the W -boson mass, while a lower limit on the values of v_R and v_S can be obtained from the consideration of the masses of heavy gauge bosons W_R and A' arising in this model. While scanning over the parameters we have set the values of v_R and v_S at their lower limits of 14.7 TeV and 13 TeV respectively.

The result of the scan is presented in Fig. 1. For the points in the plot, value of one of the eigenstates satisfies the SM Higgs mass condition and Higgs signal strength to $b\bar{b}$ decay mode [15]. It can be seen from the plot, that relatively larger values of the parameters controlling the off-diagonal terms of the mass matrix are possible. This in turn implies the eigenstates (particularly the one which can be identified with h^0) are linear combinations all three gauge states $\{h_1^0, h_R^0, h_S^0\}$. while performing this scan over a large range of parameter space, we have observed that

in most cases it keeps λ_1 more or less fixed close to the value $\frac{m_{h^0}^2}{2k_1^2}$. But the values of ρ_1 and α_1 are completely unconstrained. Instead of diagonalising the mass matrix numerically we have restricted ourselves to the values of $c_1 + c_3$ and γ_1 such that the corresponding off-diagonal terms in the mass matrix can be neglected with respect to the diagonal terms. In this limit, large values of β_1 forces one to accept large values of α_1 so that SM Higgs signal strengths as calculated from the model is in agreement with experimental observation. Furthermore, we keep a tiny value for β_1 consistent with the above scan result. Under such assumptions about the values of these parameters, mass (squared) eigenvalues can be approximated by the following expressions,

$$\begin{aligned} m_{h^0}^2 &= \lambda_1 k_1^2 + \alpha_1 v_S^2 - \sqrt{\Delta} \\ m_{H_R^0}^2 &\simeq 2\rho_1 v_R^2 \\ m_{H_S^0}^2 &= \lambda_1 k_1^2 + \alpha_1 v_S^2 + \sqrt{\Delta} \end{aligned} \quad (24)$$

with the eigenstate corresponding to the eigenvalue $m_{h^0}^2$ will be identified with the SM-like Higgs boson with mass 125 GeV. Here, $\Delta = (\alpha_1 v_S^2 - \lambda_1 k_1^2)^2 + \beta_1^2 k_1^2 v_S^2$. Mixing angle, θ , (operative between h^0 and H_S^0) in small β_1 limit, can be written as,

$$\tan(2\theta) = \frac{\beta_1 k_1 v_S}{\alpha_1 v_S^2 - \lambda_1 k_1^2} \quad (25)$$

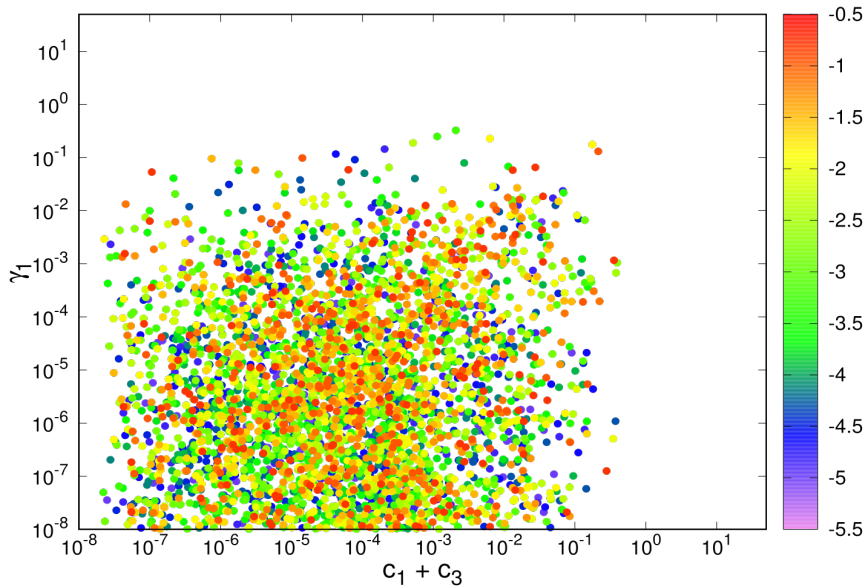


Figure 1: Allowed parameter space for $(c_1 + c_3)$ and γ_1 for some fixed values of β_1 . The side bar represents the values of β_1 in \log_{10} scale.

We will be mainly interested in a study considering in the above mentioned simplified version of the parameter space where we have only considered that H_S^0 has a tiny mixing (proportional to β_1) with SM-like Higgs boson h^0 . At the end, we will make comment about the possible outcome of a study with non-negligible values of $c_1 + c_3$ and γ_1 .

2.2 Gauge sector of $SU(3)_C \otimes SU(2)_L \otimes U(1)_L \otimes SU(2)_R \otimes U(1)_R$ model

The gauge sector of 32121 model consists of 16 gauge bosons namely, the eight gluons ($G^{a'}$, $a' = 1, \dots, 8$), $SU(2)_{L,R}$ gauge bosons, W_L^a, W_R^a , ($a = 1, 2, 3$) and two $U(1)$ gauge bosons B_L and B_R . Their interactions are governed by 5 gauge coupling constants $g_3, g_{2L}, g_{2R}, g_{1L}$ and g_{1R} .

The gauge kinetic Lagrangian can be expressed in terms of field strength tensor in usual way,

$$\mathcal{L}_{GK} = -\frac{1}{4}G^{a'\mu\nu}G_{\mu\nu}^{a'} - \frac{1}{4}W_L^{a\mu\nu}W_{L\mu\nu}^a - \frac{1}{4}W_R^{a\mu\nu}W_{R\mu\nu}^a - \frac{1}{4}B_L^{\mu\nu}B_{L\mu\nu} - \frac{1}{4}B_R^{\mu\nu}B_{R\mu\nu} - \frac{\epsilon}{2}B_L^{\mu\nu}B_{R\mu\nu} \quad (26)$$

The last term in Eq. (26) represents the $U(1)_{L,R}$ kinetic mixing proportional to a dimensionless parameter ϵ . A non-zero value of the kinetic mixing coefficient ϵ would modify the extra heavy neutral gauge boson coupling to a pair of fermions [16]. However, focus of our present study is not in that direction and we will use $\epsilon = 0$ in our following analysis.

The charged gauge bosons mass-matrix (in $W_L - W_R$ basis) follows from the Higgs kinetic Lagrangian (Eq. (5)) in $k_1, k_2 \neq 0$ limit:

$$M_{W^\pm}^2 = \frac{1}{4} \begin{pmatrix} g_{2L}^2(k_1^2 + k_2^2) & -2g_{2L}g_{2R}k_1k_2 \\ -2g_{2L}g_{2R}k_1k_2 & g_{2R}^2(k_1^2 + k_2^2 + v_R^2) \end{pmatrix} \quad (27)$$

which in small k_2 limit appears as,

$$M_{W^\pm}^2 = \frac{1}{4} \begin{pmatrix} g_{2L}^2 k_1^2 & 0 \\ 0 & g_{2R}^2(k_1^2 + v_R^2) \end{pmatrix} \quad (28)$$

Eigenvalues of the already diagonalised mass matrix provide W_L and W_R masses. The experimentally measured value of W_L mass fixes k_1 at 246 GeV, if we set at $g_{2L} = e/\sin\theta_W$ where, θ_W is the Weinberg angle. Throughout our article, we shall denote W_L as the SM W boson with a mass 80.379 GeV [15]. Experimentally measured value of W mass would fix the value of k_1 and an experimental lower limit on W_R mass [17] provides a lower bound on $v_R (> 14.7 \text{ TeV})$.

One can similarly obtain the mass matrix for neutral gauge bosons in W_{3L}, W_{3R}, B_L, B_R basis, with $k_2 \neq 0$, M_{NG}^2 :

$$\frac{1}{2} \begin{pmatrix} \frac{1}{2}g_{2L}^2 k_+^2 & -\frac{1}{2}g_{2L}g_{2R}k_+^2 & \frac{1}{6}g_{1L}g_{2L}k_-^2 & -\frac{1}{6}g_{1R}g_{2L}k_-^2 \\ -\frac{1}{2}g_{2L}g_{2R}k_+^2 & \frac{1}{2}g_{2R}^2(k_+^2 + v_R^2) & -\frac{1}{3}g_{1L}g_{2R}(\frac{1}{2}k_-^2 + v_R^2) & \frac{1}{6}g_{1R}g_{2R}(k_-^2 - v_R^2) \\ \frac{1}{6}g_{1L}g_{2L}k_-^2 & -\frac{1}{3}g_{1L}g_{2R}(\frac{1}{2}k_-^2 + v_R^2) & g_{1L}^2(\frac{1}{18}k_+^2 + \frac{2}{9}v_R^2 + \frac{2}{9}v_S^2) & g_{1L}g_{1R}(-\frac{1}{18}k_+^2 + \frac{1}{9}v_R^2 - \frac{2}{9}v_S^2) \\ -\frac{1}{6}g_{1R}g_{2L}k_-^2 & \frac{1}{6}g_{1R}g_{2R}(k_-^2 - v_R^2) & g_{1L}g_{1R}(-\frac{1}{18}k_+^2 + \frac{1}{9}v_R^2 - \frac{2}{9}v_S^2) & g_{1R}^2(\frac{1}{18}k_+^2 + \frac{1}{18}v_R^2 + \frac{2}{9}v_S^2) \end{pmatrix} \quad (29)$$

which in small k_2 scenario practically becomes,

$$M_{NG}^2 = \frac{1}{2} \begin{pmatrix} \frac{1}{2}g_{2L}^2 k_1^2 & -\frac{1}{2}g_{2L}g_{2R}k_1^2 & \frac{1}{6}g_{1L}g_{2L}k_1^2 & -\frac{1}{6}g_{1R}g_{2L}k_1^2 \\ -\frac{1}{2}g_{2L}g_{2R}k_1^2 & \frac{1}{2}g_{2R}^2(k_1^2 + v_R^2) & -\frac{1}{3}g_{1L}g_{2R}(\frac{1}{2}k_1^2 + v_R^2) & \frac{1}{6}g_{1R}g_{2R}(k_1^2 - v_R^2) \\ \frac{1}{6}g_{1L}g_{2L}k_1^2 & -\frac{1}{3}g_{1L}g_{2R}(\frac{1}{2}k_1^2 + v_R^2) & g_{1L}^2(\frac{1}{18}k_1^2 + \frac{2}{9}v_R^2 + \frac{2}{9}v_S^2) & g_{1L}g_{1R}(-\frac{1}{18}k_1^2 + \frac{1}{9}v_R^2 - \frac{2}{9}v_S^2) \\ -\frac{1}{6}g_{1R}g_{2L}k_1^2 & \frac{1}{6}g_{1R}g_{2R}(k_1^2 - v_R^2) & g_{1L}g_{1R}(-\frac{1}{18}k_1^2 + \frac{1}{9}v_R^2 - \frac{2}{9}v_S^2) & g_{1R}^2(\frac{1}{18}k_1^2 + \frac{1}{18}v_R^2 + \frac{2}{9}v_S^2) \end{pmatrix} \quad (30)$$

In practical, the presence of this small k_2 will not sensitively affect the masses and mixings in the neutral gauge sector .

Before we make predictions about the masses of the neutral gauge bosons, let us make further assumption about the four gauge coupling constants. We will identify the $SU(2)_L$ of 32121 with the weak isospin group of the Standard Model. It follows automatically that $U(1)_Y$ of the SM will arise due to breaking of $SU(2)_R \otimes U(1)_L \otimes U(1)_R$. Consequently, one can identify g_Y (the $U(1)_Y$ gauge coupling constant with $g_Y = e/\cos\theta_W$) of the SM via the following relation: .

$$\frac{1}{g_Y^2} = \frac{1}{g_{2R}^2} + \frac{1}{g_{1L}^2} + \frac{1}{g_{1R}^2} \quad (31)$$

Above relation among the gauge couplings allows us to choose any two of g_{2R}, g_{1L} and g_{1R} independently. In order to keep our Lagrangian manifestly LR symmetric, we assume $g_{2L} = g_{2R}$ and $g_{1L} = g_{1R}$. All our analysis presented in the following will be based on this assumption.

To completely determine the gauge boson masses we need to know the values of the gauge coupling constants and three non-zero vacuum expectation values (vevs). The gauge coupling constants have been already fixed from the symmetry breaking condition and demand of manifest Left-Right symmetry. The value or allowed range of values of v_S remains to be known for evaluation of the gauge boson masses from Eqs. (28), (30). It is to be noted that v_S plays a crucial role in breaking $U(1)_L \otimes U(1)_R$. The tree level relation among m_Z, m_W and $\cos\theta_W$ has been ensured by identifying the massless eigenstate (of M_{NG}^2) with the photon, which has equal coupling to left- and right-chiral fermions.

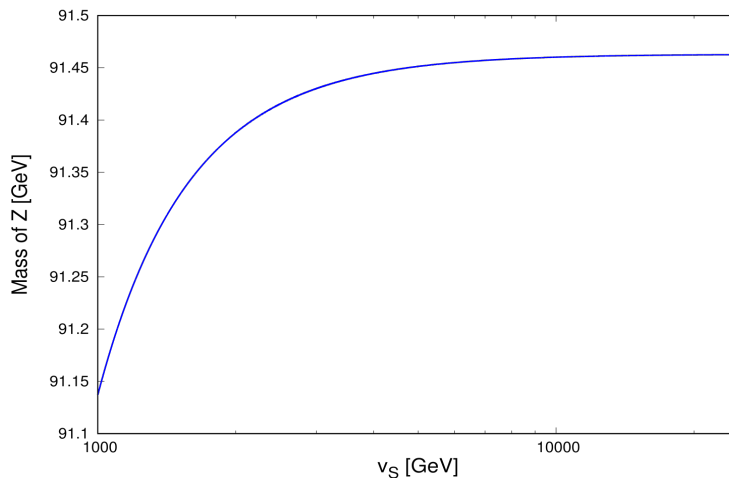


Figure 2: Weak dependence of Z mass on v_S

We have implemented the model Lagrangian in `SARAH` [19] as well as in `FeynRules` [20]. In the following analysis all the cross-sections will be calculated with help of `Madgraph5(v2.6.6)` [21] using `NNPDF23NLO` parton distribution functions [22] with the factorisation scale set equal to the average mass of the final state particles.

Upon diagonalisation, one of the eigenvalues of Eq. (30) will give a zero eigenvalue corresponding to the photon. Another eigenvalue comes out to be nearly equal to 91.2 GeV, which we identify with the Z -boson. Other two eigenvalues correspond to two heavy neutral gauge bosons which we identify as Z' and A' , the last one being a hall mark of an extra $U(1)$ gauge symmetry.

Fig. 2 shows the weak dependence of Z mass on v_S whereas, Fig. 3 reveals a strong correlation between the mass of A' with v_S . Taking a hint from this fact, we would like to find an allowed range of v_S from the LHC data itself. In such an effort, an experimental search of a heavy neutral gauge boson at the LHC and its subsequent decay to a pair of leptons would be helpful. ATLAS collaboration at the LHC [18] has looked for a pair of high p_T leptons (e and μ) to put an upper limit on the production cross-section times the branching ratio of a heavy neutral gauge boson at 13 TeV. We have translated this upper limit on the $\sigma \times BR$ to the mass of A' . In our model A' couples to both quarks and leptons with couplings proportional to their $U(1)_{L,R}$ charges. We present the $\sigma \times BR$ of A' in Fig. 4. The black solid and dashed lines represent the observed and expected 95% C.L. upper limit on cross-section times branching ratio by ATLAS respectively. While the blue solid line gives the $\sigma \times BR$ of A' in 32121 model as a function of A' mass. One can find a lower limit on A' mass equals to 3.5 TeV.

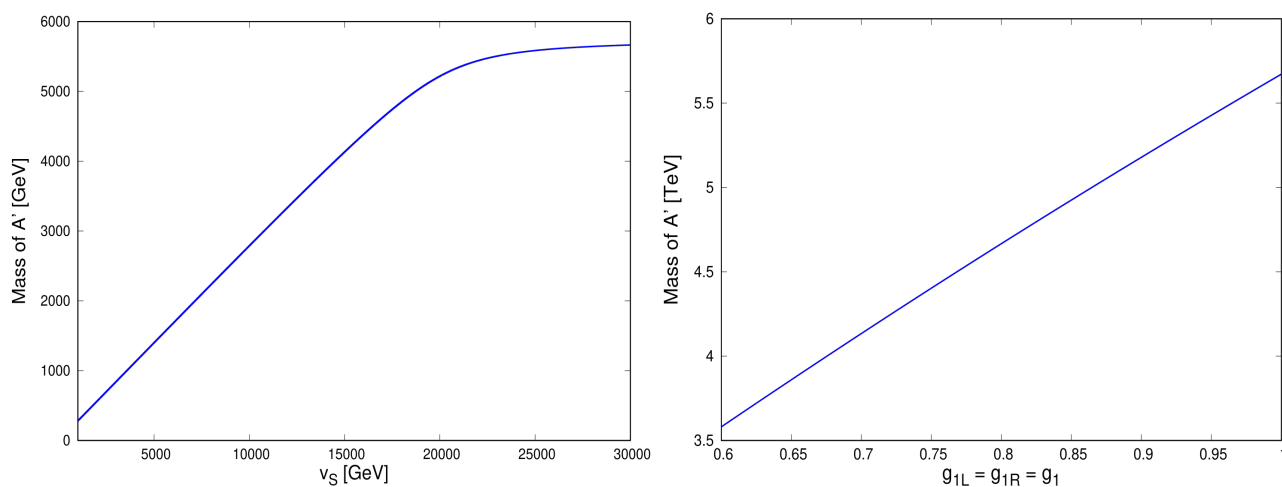


Figure 3: Dependence of A' mass on v_S (left panel) and on g_{1L} and g_{1R} , with $g_{1L} = g_{1R}$ for a fixed v_S (right panel).

Knowledge of a lower limit on A' mass enables one to get a lower limit on v_S . $m_{A'}$ is a function of the gauge coupling constants and three non-zero vevs necessary for symmetry breaking. Mass of A' has a very weak dependence on k_1 and v_R in comparison to v_S . Values of the gauge couplings and k_1 are fixed. And we set value of v_R at its lower limit while obtaining a lower limit on v_S . We thus arrive a lower limit on v_S which equals to 12.61 TeV. $m_{A'}$ is a slowly increasing function of v_R . So one cannot arrive at an absolute lower limit on v_S . The allowed region of $v_R - v_S$ space has been presented in Fig. 5.

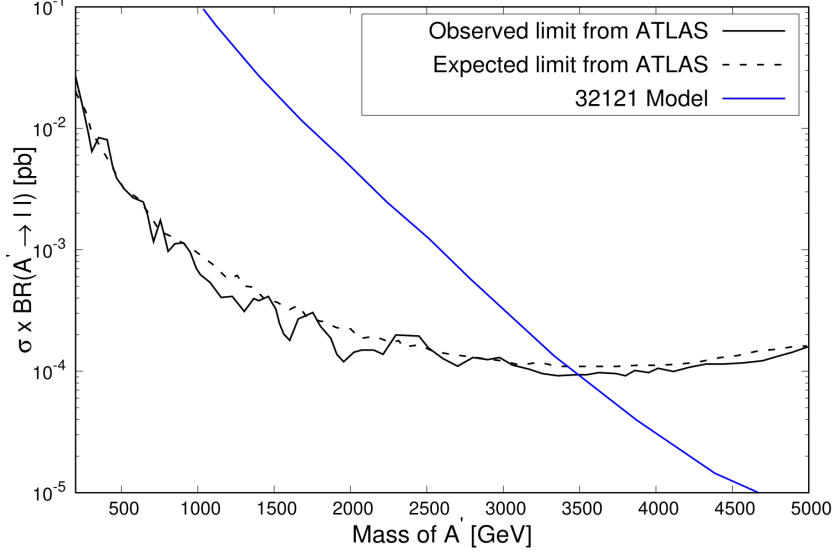


Figure 4: Production cross-section, $\sigma \times BR$ plot for a heavy neutral gauge boson production at the LHC. The black solid (dashed) line represents the observed (expected) 95% C.L. upper limit on $\sigma \times BR$ from ATLAS (with $\sqrt{s} = 13$ TeV, 36.1 fb^{-1}) considering dilepton decay channel of the produced gauge boson and the blue line corresponds to the prediction of 32121 model.

Z' mass on the other hand, is mainly controlled by v_R and it has a weak dependence on v_S . With v_R at its lower limit, Z' mass comes out to be 5.9 TeV. For such a massive Z' , cross-section times its branching ratio to a pair of leptons is of the order of 10^{-3} fb. This rate is well below the upper limit of cross-section times BR for a heavy neutral gauge boson by ATLAS collaboration [18] and presented in Fig. 4.

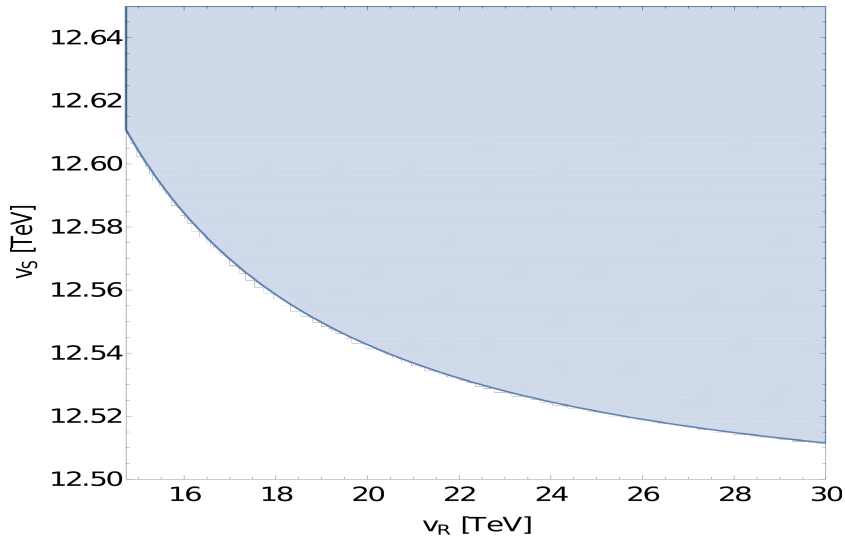


Figure 5: Allowed region in $v_R - v_S$ space, obtained from the limits on A' mass. $m_{A'}$ has a strong dependence on v_S and have a milder dependence on v_R .

2.3 Fermion sector of $SU(3)_C \otimes SU(2)_L \otimes U(1)_L \otimes SU(2)_R \otimes U(1)_R$ model

The gauge quantum numbers of the fermions have been already listed in Table 1. In the following we note the fermions with their chiral components.

$$\begin{aligned}
L_L &= \begin{pmatrix} \nu_L \\ e_L \end{pmatrix}, & L_R &= \begin{pmatrix} \nu_R \\ e_R \end{pmatrix} \\
Q_L &= \begin{pmatrix} u_L \\ d_L \end{pmatrix}, & Q_R &= \begin{pmatrix} u_R \\ d_R \end{pmatrix} \\
Q_{LS} &= q_{SL}, \quad Q_{RS} = q_{SR}, \quad L_S = l_S \quad \text{and,} \\
L_B &= \begin{pmatrix} N_1 & E_1 \\ E_2 & N_2 \end{pmatrix} \quad \text{with} \quad \bar{L}_B = \begin{pmatrix} \bar{N}_1 & \bar{E}_2 \\ \bar{E}_1 & \bar{N}_2 \end{pmatrix}
\end{aligned} \tag{32}$$

Here, L_L, L_R, Q_L, Q_R represent SM fermions along with a right-handed neutrino (ν_R). Q_{LS} and Q_{RS} are color triplets and $SU(2)$ gauge singlet exotic quarks having $U(1)_L$ and $U(1)_R$ hyper-charges respectively. They together form a 4-component Dirac spinor q_S . N_1 and N_2 are neutral heavy leptons while E_1 and E_2 are singly charged heavy leptons. They pair-wise form 4-component Dirac spinors, N and E respectively. l_S is a neutral exotic singlet fermion but carrying $U(1)_L$ and $U(1)_R$ gauge quantum numbers.

The fermionic sector of this model consists of several heavy leptons and quarks apart from their SM counterparts. We would like to spend few words on them. The presence of ν_R facilitates us to write a Dirac or Majorana mass for the neutrinos [6], [23]⁵. Heavy charged lepton E^\pm and heavy neutrino N arise from the $SU(2)$ bi-doublet L_B . These will couple to SM gauge bosons and thus can be produced at the LHC. Similarly, $SU(2)$ singlet quarks Q_{LS} and Q_{RS} form a heavy quark of electric charge $+\frac{1}{3}$ of Dirac type. Finally, there remains a $SU(2)_{L,R}$ singlet lepton of zero electric charge. This could well be a candidate for Dark Matter. The assignment of $U(1)$ charges for the fermions, from the requirement of anomaly cancellation, is such that the exotic fermions can only couple to the gauge bosons but do not have any mixing with the SM fermions. This feature will play a crucial role in determining the possible signatures of these fermions at colliders.

Fermions get their masses via their interactions with Higgs fields. The relevant Yukawa Lagrangian is noted below.

$$\begin{aligned}
\mathcal{L}_{Yukawa} &= y_{qij} \bar{Q}_{iL} \Phi_B Q_{jR} + \tilde{y}_{qij} \bar{Q}_{iR} \tilde{\Phi}_B Q_{jL} + y_{lij} \bar{L}_{iL} \Phi_B L_{jR} + \tilde{y}_{lij} \bar{L}_{iR} \tilde{\Phi}_B L_{jL} \\
&+ y_{sij} \bar{Q}_{iLS} \Phi_S Q_{jRS} + y_{LBij} \text{Tr} \left[\bar{L}_{iB} \tilde{L}_{jB} \right] \Phi_S^c + \frac{y_{LSij}}{\Lambda} \bar{L}_{iS} L_{jS} \Phi_S \Phi_S \\
&+ y_{BBij} \text{Tr} \left[\bar{L}_{iB} \tilde{\Phi}_B \right] L_{jS}^c + H.C.
\end{aligned} \tag{33}$$

where, $i, j = 1, 2, 3$ are generation numbers and $y(s)$ are Yukawa coupling constants. Φ_S^c is complex conjugate of Φ_S and $\bar{L}_B = \sigma_2 L_B^* \sigma_2$.

In general the Yukawa coupling matrices, y_q, y_l, y_{LB}, y_s are non-diagonal⁶. The diagonalisation of the Yukawa matrices in the first line of Eq. 33 will give rise to the SM-fermion masses and mixing in the form of V_{CKM} and V_{PMNS} . There are no term present in the Yukawa Lagrangian leading to exotic fermion SM-fermion mixing. Thus while considering the phenomenology of the some of the exotic fermions, we have used their physical masses as the free parameters of the analysis and derive possible bounds on them from LHC itself. The last term in Eq. 33 introduces a mixing between the singlet lepton and the neutral lepton from the bi-doublet. In this work, we shall not be investigating the phenomenological implications of this term.

It is important to note a dimension-4 mass term for the singlet lepton L_S (a Weyl spinor) cannot be written as it transform non-trivially under $U(1)_{L,R}$. Using the singlet Higgs field Φ_S , we are able write a dimension-5 operator, which in turn generates mass for L_S . It is well known that any one of the Higgs bosons from **27**-plet of E_6 cannot give mass to L_S . To generate a mass using Higgs mechanism, one must employ a Higgs from a multiplet of E_6 other than **27** [25]. So Λ may be identified with the vev of such a Higgs boson. Or we can simply assume that L_S has acquired mass from a Higgs belonging to other rep. of E_6 and we treat its mass as a free parameter in our analysis.

⁵We have only noted down a possible Dirac mass term for the neutrinos in Eq. (33)

⁶In general, in an unifying model like E_6 , all the Yukawa couplings at the low energy will be generated from a single (and possibly a non-diagonal) Yukawa texture at the GUT scale [24].

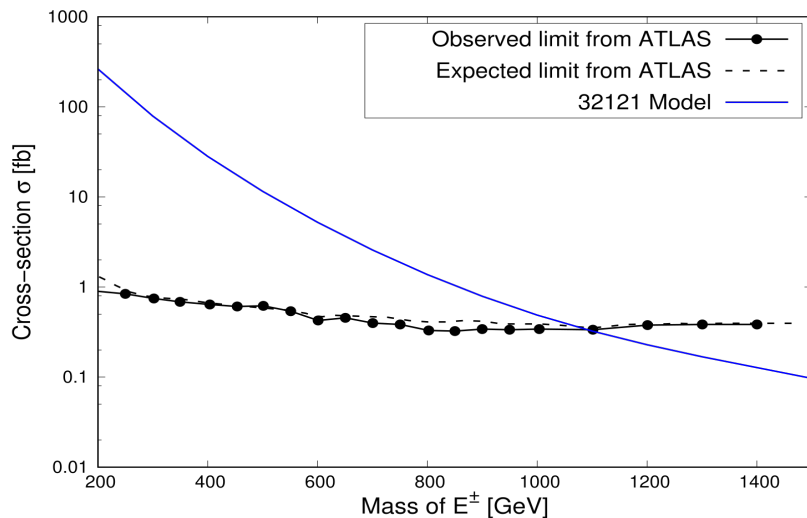


Figure 6: Observed (line with dots) and expected (dashed) 95% C.L. experimental upper limit on the cross-section (σ) of heavy charged lepton pair-production at the 13 TeV run of the LHC. Also shown in the plot the theoretical prediction from the 32121 model (blue line).

One can constrain the masses/Yukawa couplings of exotic quarks and leptons from the direct search limits on their masses at the LHC [26, 27]. As for example, ATLAS collaboration has searched for long-lived heavy charged lepton at 13 TeV run with a collected luminosity of 36.1 fb^{-1} . We have estimated the pair-production cross-section of E^+E^- at the 13 TeV and compared it with the experimental 95% C.L. upper limit on the same cross-section obtained by ATLAS collaboration. The plots have been presented in Fig. 6. One can see that E mass in 32121 model cannot be less than 1.091 TeV at 95% C.L.

3 Phenomenology of new Higgs bosons of 32121 model at the LHC

Apart from the SM-like Higgs boson, 32121 model contains a number of neutral and charged scalar states. We will now discuss the possible interactions and signatures of such states at the LHC in this section.

3.1 Phenomenology of the scalars arising from the bi-doublet in 32121 model

h_2^0 (ξ_2^0) is the neutral CP-even (odd) scalar originating from the Higgs bi-doublet, Φ_B . From Eqs. (19) and (20), we can easily see their masses are equal. They do not decay to a pair of gauge bosons as the vev k_2 has been set to zero. For the very same reason, h_2^0 or ξ_2^0 does not couple to a pair of any other scalars.

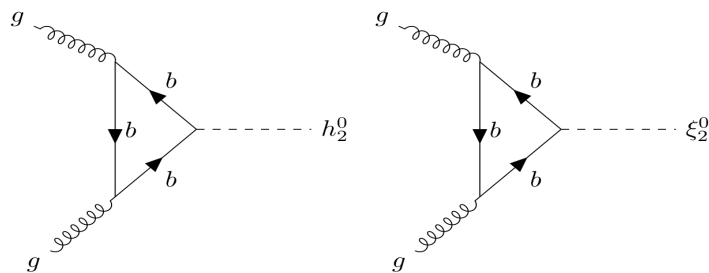


Figure 7: Feynman diagrams for h_2^0 and ξ_2^0 production via gluon gluon fusion through b quark loop

h_2^0 (ξ_2^0) couples to a pair SM fermions via Yukawa coupling (see Eq. (33)). It is interesting to note that the

coupling of h_2^0 (ξ_2^0) to a pair of top quark is proportional to bottom-Yukawa coupling and vice-versa. ATLAS and CMS have searched for a heavy neutral Higgs boson produced in association with b quarks followed by its decay to a pair of b quarks at $\sqrt{s} = 13$ TeV [29, 30]. We consider the production of an h_2^0 in association with a pair of b quarks and its decay to a pair of b quarks. The resulting rate of events can be compared with the measured rate by ATLAS Collaboration to set a lower limit on the mass of h_2^0 (ξ_2^0). The calculated (in 32121 model) and (95% C.L. upper limit on the) measured cross-sections are presented in the Fig. 8. The 95% C.L. lower limit on $m_{h_2^0/\xi_2^0}$ comes out to be greater than 800 GeV. While estimating the h_2^0 (ξ_2^0) production cross-section in association with a pair of b -quarks, we have incorporated the QCD K-factor (~ 1.1) following the ref. [31, 32]. However, the lower limit derived in the above, depends on the charged Higgs boson (H_1^\pm) mass in the following way. A careful look into the branching ratios of h_2^0 reveals that it dominantly decays to a pair of b -quarks, unless a decay to $H_1^\pm W^\mp$ is kinematically allowed,. Consequently, mass of H_1^\pm plays a crucial role in determining the rate of $4b$ final state from considered above. A heavier charged Higgs (when $h_2^0 \rightarrow H_1^\pm W^\mp$ is disallowed) will push the lower limit on h_2^0 mass in upward direction and vice versa.

In Fig. 8, we have presented the $\sigma(pp \rightarrow b\bar{b}h_2^0) \rightarrow b\bar{b}(b\bar{b})$ in two cases. The red line represents the rate when $m_{H_1^\pm} > m_{h_2^0}$ and the later decays to a pair of $b\bar{b}$ with 100% BR. While the blue curve represents the case when h_2^0 can also decay to H_1^\pm thus having a reduced decay rate to $b\bar{b}$. A charged Higgs mass of 750 GeV has been assumed while making this plot. The sudden change in the slope of the blue curve due to onset of $h_2^0 \rightarrow H_1^\pm W^\mp$ decay mode around $m_{h_2^0} \simeq 850$ GeV (see Fig. 9) is evident.

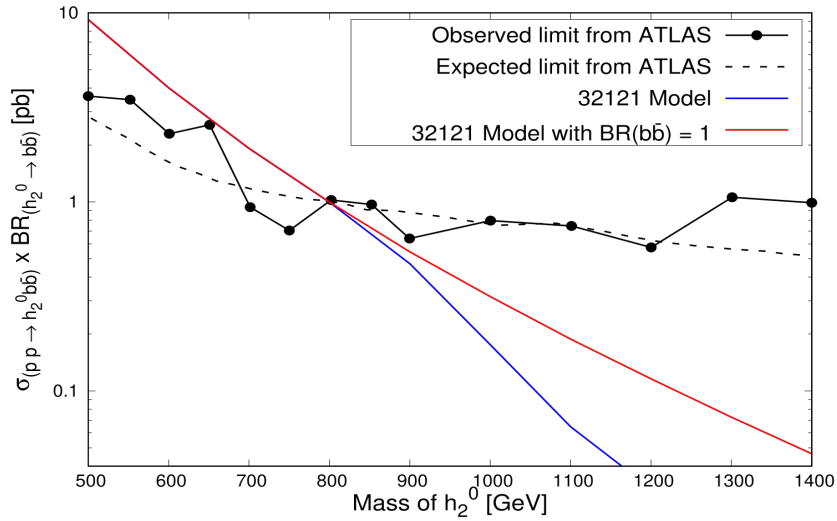


Figure 8: The black solid (dashed) line represents the observed (expected) 95% C.L. upper limit on the production cross-section (σ) times branching ratio to $b\bar{b}$, of heavy neutral Higgs boson in association with b quarks as a function of Higgs boson mass at $\sqrt{s} = 13$ TeV with 27.8 fb^{-1} integrated luminosity. The blue line corresponds to $\sigma(pp \rightarrow h_2^0 b\bar{b}) \times BR(h_2^0 \rightarrow b\bar{b})$ whereas the red line represents the same but considering $m_{H_1^\pm} > m_{h_2^0}$.

A dominant production mechanism for such a Higgs boson at the LHC will be via gluon gluon fusion (Fig. 7). Unlike the SM Higgs boson, in this case, gluon gluon fusion cross-section is dominated by the bottom quark loop. We present the production cross-section (considering NLO QCD correction for this production process, see [33]) and decay branching ratios of h_2^0 in Fig. 9.

At the 14 TeV run of the LHC, h_2^0 production cross-section varies from 14 fb for $m_{h_2^0} = 800$ GeV to 0.2 fb for 1.5 TeV mass of this scalar. Production cross-section at 27 TeV is even higher and it varies from 77 fb at $m_{h_2^0} = 800$ GeV to 1.5 fb for $m_{h_2^0} = 1500$ GeV. Once produced, h_2^0 dominantly decays to a pair of b -quarks, unless it decay to $H_1^\pm W^\mp$. The later decay mode will only be allowed when $m_{h_2^0}$ is sufficiently higher than $m_{H_1^\pm} + m_W$. This choice of mass ordering depends on the choice of parameters namely λ_3 and $c_4 - c_3$. In the plot presented in Fig. 9, a certain choice of these parameters have been assumed, so that the $h_2^0 \rightarrow H_1^\pm W^\mp$ has been kinematically allowed, with an additional assumption about the mass of H_1^\pm (750 GeV).

In the pseudo-scalar sector, ξ_2^0 arises from the Higgs bi-doublet and has a mass equal to the mass of h_2^0 . It

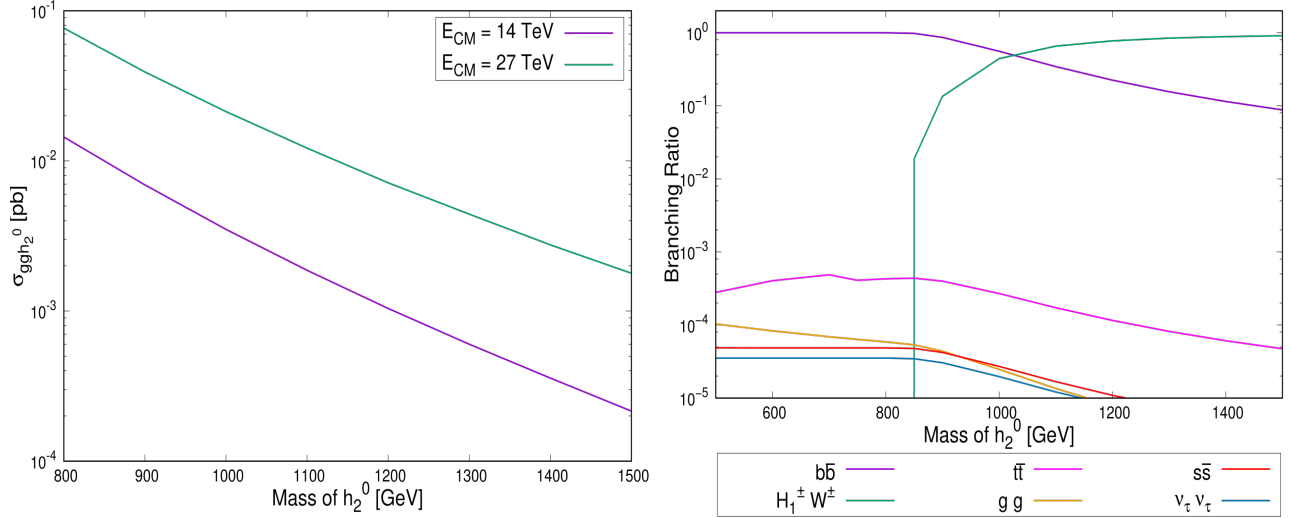


Figure 9: h_2^0 production cross section (σ) via gluon fusion at LHC (left panel) for 14 and 27 TeV proton proton center of mass energy. The right panel shows the branching ratios of h_2^0 to different final states. h_2^0 and ξ_2^0 have the same masses and coupling strengths

has exactly the similar coupling strengths to the SM fermions as the h_2^0 . The choice of vanishing k_2 forbids its coupling to a pair of gauge bosons or the scalars. Consequently the production and decay mechanism and their rate of ξ_2^0 is exactly the same as h_2^0 . We will not present these numbers separately.

Charged Higgs boson, H_1^\pm arises from the Higgs bi-doublet, Φ_B . From the expression (21), one can see, $m_{H_1^\pm}^2 = \frac{1}{2}(c_4 - c_3)(k_1^2 + v_R^2)$. This massive charged Higgs couples to SM fermions and decays to a top and a bottom quark with nearly 100% branching ratio. It also couples to the heavy gauge bosons of 32121 model but the coupling of H_1^\pm to the SM gauge bosons (W^\pm, Z) is proportional to k_2 , hence identically vanishes. It can be singly produced at LHC with a top and bottom quark or pair-produced via Drell-Yan process or via vector boson fusion process.

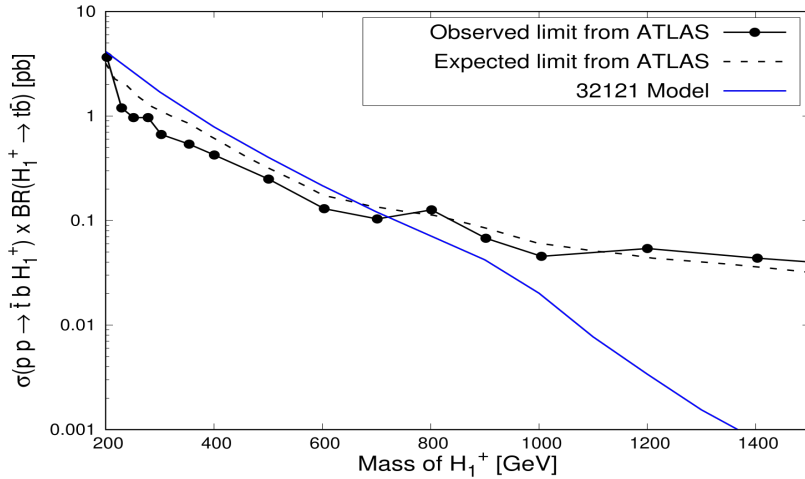


Figure 10: The black solid and dashed line represent observed and expected 95% C.L. experimental upper limit on the cross-section (σ) times BR of heavy charged scalar production via $pp \rightarrow \bar{t}bH_1^+ \times BR(H_1^+ \rightarrow t\bar{b})$ at the 13 TeV run of the LHC with 139 fb^{-1} integrated luminosity [34]. Also shown in the plot the theoretical prediction of $\sigma \times BR$ for H_1^+ production in the 32121 model (blue line).

In Fig. 11, we have presented the cross-section of associated production of H_1^\pm with a top and a bottom at the LHC and branching ratio of H_1^\pm . In case of H_1^\pm production, the main contribution will be from $gg \rightarrow \bar{t}bH_1^\pm$. ATLAS and CMS collaborations have searched for a heavy charged Higgs boson decaying to a top and bottom at 13 TeV run [34–36]. Using the most recent upper limit on the $\sigma \times BR$ provided by ATLAS, we put a lower limit on the mass of the charged Higgs $m_{H_1^\pm} > 720$ GeV (see Fig. 10). The sudden change in the slope of the blue curve representing $\sigma(pp \rightarrow \bar{t}bH_1^+) \times BR(H_1^+ \rightarrow \bar{t}b)$ is due to the sudden decrease of $BR(H_1^+ \rightarrow \bar{t}b)$ around $m_{H_1^\pm} = 900$ GeV (see Fig. 11). We have set the mass of h_2^0 (ξ_2^0) at its lower limit of 800 GeV following the Fig. 9 corresponding to the scenario when $m_{H_1^\pm} > m_{h_2^0}$ (the red line).

We have presented cross-section for $H^\pm tb$ production (in this process NLO QCD correction and running mass for b quark can be important, see [32,37]) at centre of mass energies of 14 and 27 TeV. In Fig. 11, the right panel shows the branching ratios of H_1^\pm to different final states. Until kinematically allowed for the decay to $h_2^0 W^+$ and $\xi_2^0 W^+$, H_1^+ dominantly decays to $\bar{t}b$ ($BR(H_1^+ \rightarrow \bar{t}b) \sim 0.999$). For large $m_{H_1^\pm}$ the branching ratios to h_2^0 (ξ_2^0) W^+ channel become more dominant.

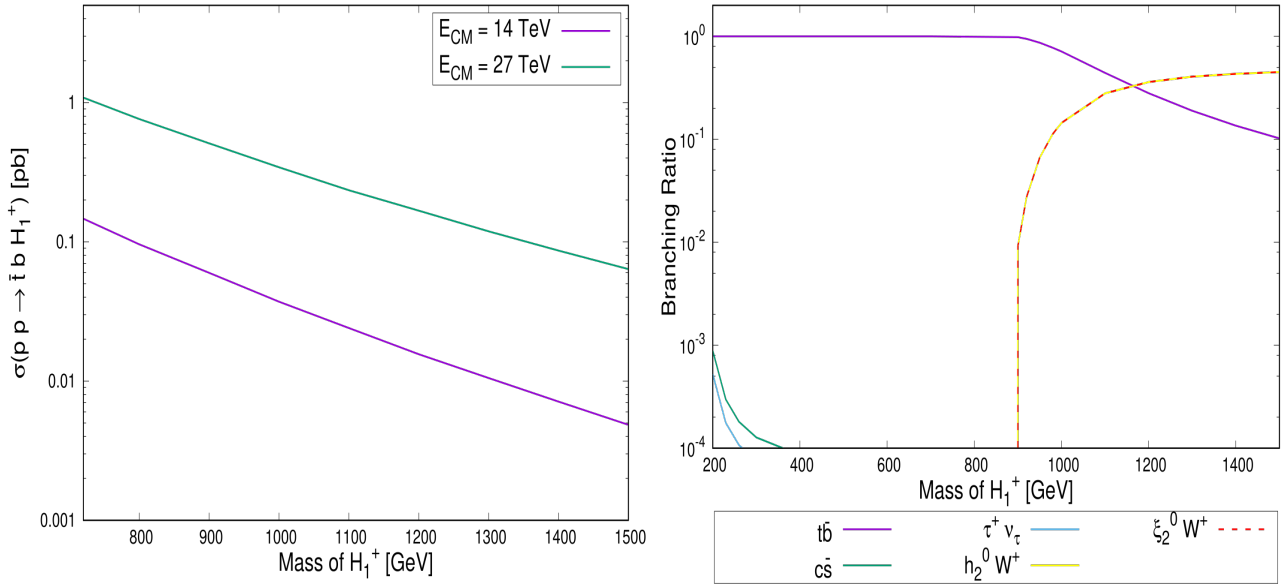


Figure 11: H_1^\pm production cross-section (σ) via $pp \rightarrow \bar{t}bH_1^+$ process at LHC (left panel) for 14 and 27 TeV proton proton center of mass energy. The right panel shows the branching ratios of H_1^\pm to different final states setting the mass of h_2^0 (ξ_2^0) at its lowest limit (800 GeV).

The cross-section for $H^\pm tb$ production at centre of mass energy approximately 14 (27) TeV varies from 0.15 (1) pb for $m_{H_1^\pm} = 720$ GeV to 0.005 (0.06) pb for $m_{H_1^\pm} = 1500$ GeV. After being produced, H_1^\pm will decay further and considering respective decay channels (e.g., tb or h_2^0 (ξ_2^0) W^\pm) one can expect a good amount of events at HL-LHC. However, one needs to consider further decays of top or h_2^0 (ξ_2^0).

3.2 Phenomenology of the scalars arising from Left-handed Higgs Doublet

In this section, our primary concern will be the neutral and charged states originating from the left-handed doublet scalar. Among the neutral CP-even scalar h_L^0 , neutral CP-odd scalar ξ_L^0 and charged scalars H_L^\pm , The first two have equal masses (see Eqs. (19), (20), (21)) and do not mix with other neutral states. These three states can be pair-produced at the LHC via quark anti-quark fusion mediated by one of the electroweak gauge bosons. However as we set v_L to be zero, neither of these states decays to a pair of SM particles.

As already pointed out, we will not vary all the parameters of the mass matrix independently to study the masses of the scalars. We will treat the physical masses as free parameters of our analysis. However some caveats are to be imposed on some combinations of parameters of the mass matrices. As for example, $\rho_3 - 2\rho_1$ will always assumed to be a positive quantity which is ascertained from the positivity of charged Higgs boson (H_L^\pm) mass

(squared). Now the other charged Higgs boson (H_1^\pm) mass squared is proportional to $c_4 - c_3$. This in turn forces us to take this combination also to be positive. As a consequence, masses of h_L^0 and ξ_L^0 are always greater than mass of H_L^\pm . However, $(m_{h_L^0} - m_{H_L^\pm})$ can be controlled by choosing a proper magnitude of the combination $(c_4 - c_3)^{\frac{k_1^2}{2}}$. From the expressions (19) and (21), $m_{h_L^0}^2 = (c_4 - c_3)^{\frac{k_1^2}{2}} + m_{H_L^\pm}^2$. We will see in the following that h_L^0 will decay to $H_L^\pm W^-$ if kinematically allowed. So in order to make h_L^0 stable, one needs to set $(c_4 - c_3)^{\frac{k_1^2}{2}} < m_W^2 + 2m_W m_{H_L^\pm}$. However, an unstable h_L^0 implies that the mass of H_1^\pm becomes too heavy in the ballpark of 17 TeV.

In the following analysis, h_L^0 and ξ_L^0 are assumed to be stable. Thus they could be potential candidates for DM. H_L^\pm also do not have any decay mode. Once produced at colliders, it passes through the detector without decaying. However being a charged particle, it leaves its signature in the tracker and e. m. calorimeter before leaving the detector. ATLAS collaboration has searched for long-lived stau ($\tilde{\tau}$, the super-symmetric partner of τ -lepton) which are very similar to the H_L^\pm [27]. So the upper limit of the cross-section of pair-production of such long-lived $\tilde{\tau}$ s at LHC centre of mass energy of 13 TeV, as quoted by ATLAS collaboration can be used in our case to constrain the $m_{H_L^\pm}$ which is the only free parameter that controls the H_L^\pm pair-production. In Fig. 12, we present the variation of H_L^\pm pair-production cross-section (blue solid line) as a function of its mass. Over-layed are the observed and expected upper limits on the pair-production of long-lived stau (black solid and dashed lines). The intersection of these two curves gives us a 95% C.L. lower limit of 494 GeV, on the left-handed charged Higgs boson (H_L^\pm) mass.

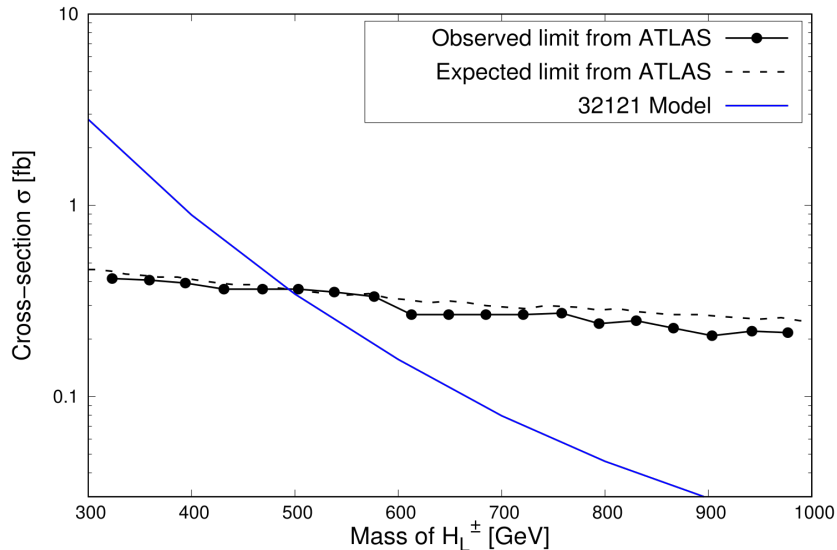


Figure 12: Observed (line with dots) and expected (dashed) 95% C.L. experimental upper limit on the cross-section (σ) of heavy stable charged scalar pair-production at the 13 TeV run of the LHC. Also shown in the plot the theoretical prediction for $H_L^\pm H_L^\mp$ pair-production cross-section in the 32121 model (blue line).

Let us now concentrate on the possible production and decay signatures of charged and neutral Higgs bosons arising from the left-handed doublet. As mentioned above, these can be pair-produced at the LHC, via a mechanism similar to Drell-Yan. In Fig. 13, the pair-production cross-sections have been presented with Higgs masses at 14 (27) TeV run of LHC. One can see from Fig. 13, production cross-section for H_L^\pm varies from 0.4 (1.8) fb at 500 GeV to 0.005 (0.06) fb at 1.5 TeV at the center of mass energy 14 (27) TeV. H_L^\pm being stable, does not decay any further and we are left with two ionising tracks of heavy particle in the detector [27], [28]. At HL-LHC, such a cross-section results into 15 background free events even for a H_L^\pm mass of 1.5 TeV. This particular signature is unique and cannot arise from the SM. Thus we hope to explore stable charged Higgs masses upto 1.5 TeV at the 14 TeV HL run of LHC.

We now turn to the production of a H_L^\pm in association with either a h_L^0 or ξ_L^0 . The production mechanism at the LHC is same as above but with a small difference. The scalar current in the later case is connected to initial state left-handed quark current by a W^\pm propagator. Consequently the cross-section for $h_L^0 H_L^\pm$ is lower than the

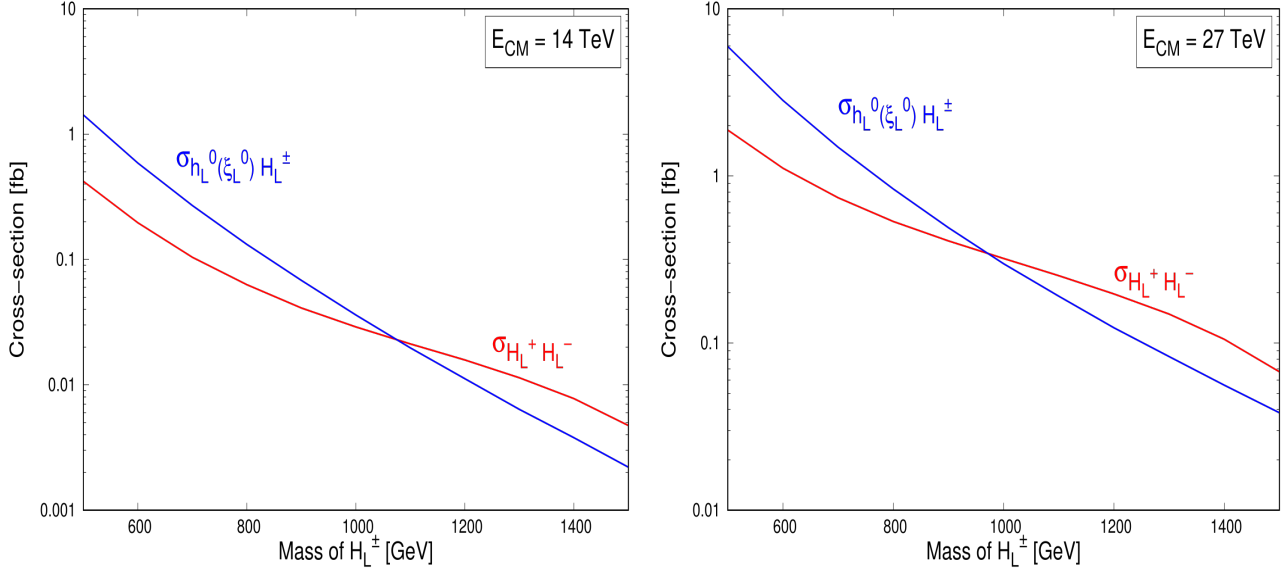


Figure 13: The red solid line corresponds to H_L^\pm pair-production cross-section (σ) at LHC at $\sqrt{s} = 14$ TeV (left panel) and at $\sqrt{s} = 27$ TeV (right panel) whereas the blue solid line represents the combined production cross-section of one charged (H_L^\pm) and one neutral (CP-even or CP-odd) scalar at LHC at $\sqrt{s} = 14$ TeV (left panel) and at $\sqrt{s} = 27$ TeV (right panel)

H_L^\pm pair-production. However, when we combine the $\xi_L^0 H_L^\pm$ with it, total cross-section of associated production becomes comparable with pair-production rate of charged Higgs bosons. In Fig. 13, associated production cross-section has been presented. One can see that at 14 (27) TeV run of LHC, the cross-section varies from 1.4 (5.9) fb to 0.002 (0.038) fb when the charged Higgs mass varies from 0.5 TeV to 1.5 TeV.

While discussing the possible signatures of the associated production, we have to be careful about the mass ordering between H_L^\pm and h_L^0 (ξ_L^0). When kinematically allowed, h_L^0 will decay (with 100% branching ratio) to $W^- H_L^\pm$. Depending the further decay of the W -boson, associated production will result into two charged tracks + 2 jets or 2 charged tracks with a lepton and \cancel{E}_T . On the other hand when h_L^0 is stable, associated production would result into a signal, comprising of a single charged track (from H_L^\pm) in association with \cancel{E}_T (arising from h_L^0 and ξ_L^0).

3.3 Phenomenology of the scalar arising from Right-handed Higgs Doublet

Next, in our agenda, is the heavy neutral Higgs boson, H_R^0 . Due to non-zero v_R , it couples to a pair of neutral heavy gauge bosons. But it cannot have any coupling to SM fermions⁷. The plot (Fig. 14) showing the branching ratios of H_R^0 reveals that it dominantly decays to a pair of SM Higgs bosons or to a pair of H_L^\pm or h_L^0 (ξ_L^0) once these decays are kinematically allowed. Decay to a pair of heavy neutral gauge bosons are kinematically disallowed. Furthermore, coupling of H_R^0 to a pair of Z bosons conspires to be small hence its decay rate to a pair Z bosons is negligible. H_R^0 can have an effective coupling at one-loop (H_L^\pm , W_R^\pm and H_1^\pm running in the triangle loop) to a pair of photons. The decay branching ratio can be as high as 10^{-5} over a wide mass range of H_R^0 , and is thus not phenomenologically very interesting.

The main production mechanism for H_R^0 is in association with a gauge boson (Z , Z' , A' and W_R) via annihilation of quark anti-quark pair. It can also be produced in vector boson fusion mechanism. In this article, we will only consider the production of H_R^0 in association with a vector boson (Fig. 15).

In Fig. 14 (right panel) we have presented the combined cross-section of production of a H_R^0 in association with Z' , A' and W_R , with the heavy gauge boson masses set at their experimental lower limits. Among these three production channels, contribution of $\sigma(H_R^0 A')$ is nearly 70% of combined cross-section presented in Fig.

⁷It may couple to the SM fermions if we allow a possible mixing between H_R^0 with SM Higgs boson

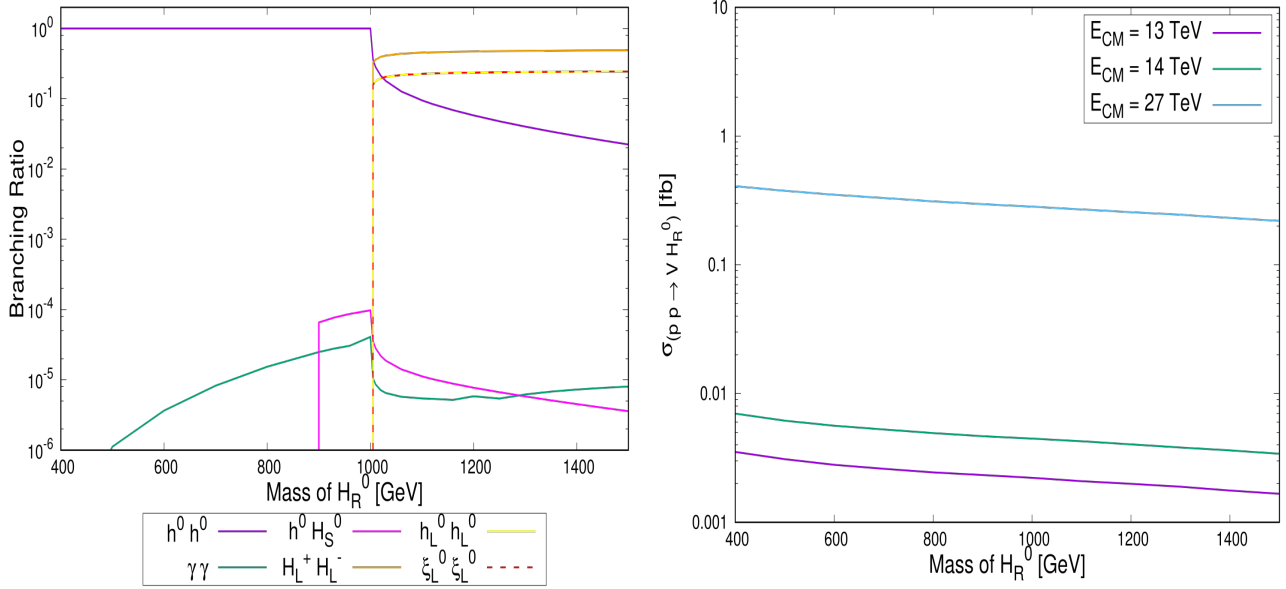


Figure 14: Associated production cross section (σ) of H_R^0 along with a vector boson at LHC (left panel) for 13, 14 and 27 TeV proton proton center of mass energy. The right panel shows the branching ratios of H_R^0 to different final states with an assumption of $m_{h_L^0} = m_{\xi_L^0} = 500$ GeV and $m_{H_S^0} = 700$ GeV.

14. Combined cross-section of H_R^0 associated production at the LHC varies from 0.4 fb to 0.22 fb for a range of m_{H_R} : 400 to 1500 GeV at a center of mass energy of 27 TeV. At 14 TeV run of the LHC, the cross-section is quite small. It is in the ballpark of 0.005 fb (Fig. 14) for a H_R^0 of 1 TeV mass. The kinematic suppression due to the presence of a heavy gauge boson in the final state can be one of the reasons behind the smallness of the total cross-section.

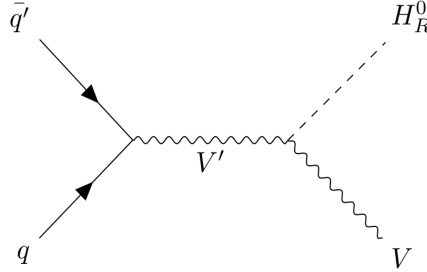


Figure 15: Feynman diagram for H_R^0 production in association with a vector boson where V, V' represent any vector boson of 32121 model (Z, Z', A' and W_R).

Before we close this sub-section, let us make some brief comments about the possible signature of H_R^0 at the LHC. The most promising, signature, in our opinion will arise when H_R^0 can decay to a pair of H_L^\pm . As mentioned before, if will produce two charged tracks in the detector with their invariant mass peaking at the mass of H_R^0 . Along with a pair of charged tracks heavy gauge boson decay will probably give rise to a pair of high mass jets or leptons. As for example, at 27 TeV run of the HL-LHC, one expects around 30 two charged tracks two lepton events for a $m_{H_R^0} = 1$ TeV⁸. While at the 14 TeV run with high luminosity option, detection of such events seems

⁸The branching ratio for di-lepton decay (e, μ, τ) of A' is $\sim 10\%$ and branching ratio of $H_R^0 \rightarrow H_L^+ H_L^-$ is around 50%. So considering almost 70% contribution of $\sigma(H_R^0 A')$, at 27 TeV run with 3000 fb^{-1} integrated luminosity, for the process $\sigma(pp \rightarrow H_R^0 A') \times BR(A' \rightarrow l) \times BR(H_R^0 \rightarrow H_L^+ H_L^-)$ one can expect around 30 events for 1 TeV H_R^0 mass.

to be very challenging even for a 500 GeV H_R^0 .

3.4 Phenomenology of the $SU(2)_L \otimes SU(2)_R$ Singlet scalar in 32121 model

Next, in our agenda, is the scalar arising from $SU(2)_L \times SU(2)_R$ singlet Φ_S . β_1 being small in order to satisfy the SM Higgs bosons signal strength (see Fig. 1), it does not have any significant role in the phenomenology of the singlet scalar and we can treat mass of the singlet scalar itself as the free parameter of our analysis. In the following we intend to study the decays and dominant production channel of the singlet scalar boson.

In Fig. 16, we present branching ratios of H_S^0 to its available decay channels. To remind, WW , ZZ , $t\bar{t}$, $b\bar{b}$ decays of H_S^0 take place via the mixing with the SM Higgs boson. While rest of the decays are driven via the direct couplings of H_S^0 to the decaying particles.

The dominant contribution to $H_S^0 \rightarrow gg, \gamma\gamma$ decay, arise from triangle loops of heavy exotic quarks and leptons. Charged Higgs states arising from Φ_B, Φ_L also contribute to singlet Higgs decay to $\gamma\gamma$. $H_S^0 \rightarrow gg$ is important as production cross-section of H_S^0 via gluon fusion is directly proportional to this decay width. However, v_S being large, singlet Higgs Yukawa to exotic leptons/quarks are tiny (see Eq. (33) in section 2.3). Consequently, decay width to gg is small. Similar arguments can be given to understand the smallness of $H_S^0 \rightarrow \gamma\gamma$ decay rate.

The branching ratios to several decay channels are moderately sensitive to β_1 . With a higher value of β_1 ($\sim 10^{-3}$) one can satisfy all the constraints from SM Higgs boson signal strengths. However, $\beta_1 > 10^{-3}$ ⁹ will lead to a singlet Higgs boson mass of 700 GeV and above. Furthermore, a higher value of β_1 leads to a larger mixing between the singlet and the SM-like Higgs boson. Thus the singlet Higgs boson decay rates to $t\bar{t}$, $b\bar{b}$, WW and ZZ channels will increase slightly. The variation of branching ratios over a wide mass range of H_S^0 for a fixed β_1 have been shown in the Fig. 16.

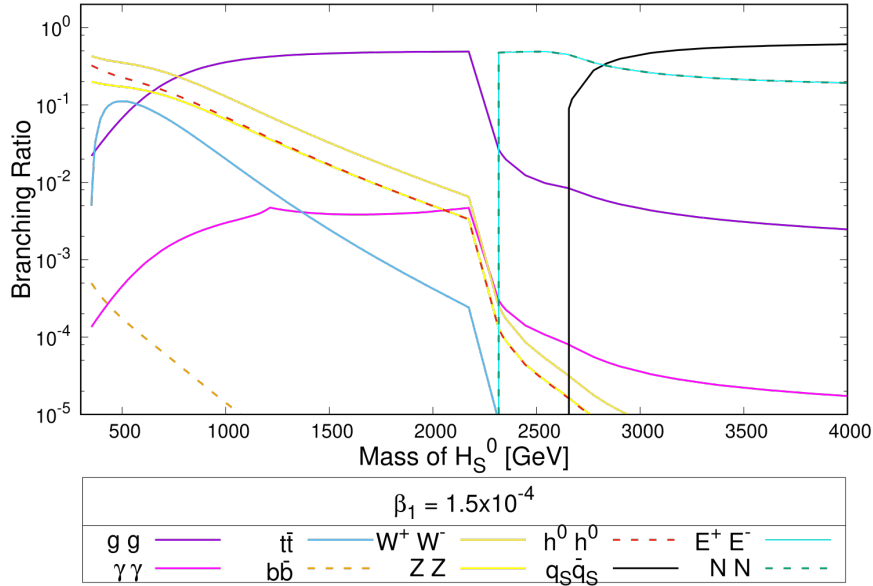


Figure 16: Branching ratio of H_S^0 to different channels including exotic quarks and exotic leptons for $\beta_1 = 1.5 \times 10^{-4}$ and $v_S = 13$ TeV and exotic quark mass 1.3 TeV.

In this section we present singlet Higgs production cross-section via gluon gluon fusion over a range of singlet Higgs mass. The production mechanism is the same as the SM Higgs production via gluon fusion. However, the triangle loop (see Fig. 17) is driven by exotic quarks which are heavy in mass. There will be a very tiny contribution from the standard model top-quark through the mixing of singlet Higgs with the SM Higgs boson. While estimating this cross-section we have incorporated a K-factor following ref. [33], assuming higher order QCD correction to the production of a singlet Higgs boson will be of similar order that of a SM Higgs boson production via gluon fusion. For our illustration we have assumed β_1 (mixing parameter) to be equal to 1.5×10^{-4} . This value of β_1 is consistent with the measured values of SM Higgs boson signal strengths to different channels.

⁹ $\beta_1 > 0.01$ is excluded as the singlet component in SM-like Higgs will be too high to satisfy the experimentally measured signal

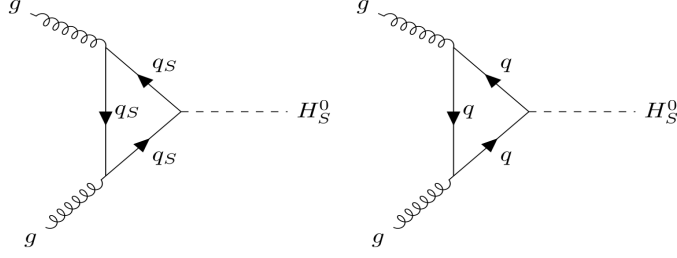


Figure 17: Feynman diagram for H_S^0 production via gluon gluon fusion quark loops, q_S is the exotic singlet quark and q represents any SM quark

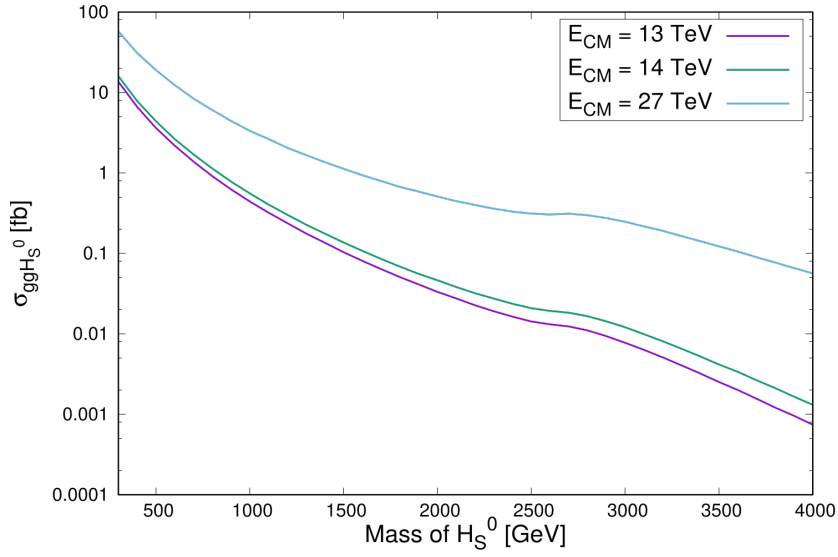


Figure 18: H_S^0 production cross-section (σ) via gluon fusion for $\beta_1 = 1.5 \times 10^{-4}$ and $v_S = 13$ TeV and exotic quark mass 1.3 TeV.

In Fig. 18, we have presented the singlet Higgs boson production cross-section at proton proton centre of mass energies 13, 14 and 27 TeV respectively. At 14 (27) TeV run of LHC, production cross-section varies from 15.9 (57.6) fb to 10^{-3} (0.056) fb when H_S^0 mass changes from 0.3 to 4 TeV. Although the production mechanism is similar to the SM Higgs boson production via gluon fusion, the cross-section for H_S^0 production is order of magnitude smaller than a SM-like Higgs boson of same mass, even after considering the contribution from 3 species of $SU(2)$ singlet exotic quarks. This can be explained by the small Yukawa coupling of these exotic quarks to the Singlet Higgs boson (see Eq. (33)). We have assumed the exotic quark mass to be equal to 1.3 TeV [26]¹⁰. Before we conclude, let us make some qualitative comments about the possible signatures of H_S^0 at the LHC. For a low mass (< 700 GeV), WW decay mode can be exploited to look for possible signatures of this Higgs boson. However, once, $m_{H_S^0}$ becomes greater than a TeV, gluon gluon decay of H_S^0 becomes dominant and detection of such a scalar will be difficult due to a possible large QCD background. However, for higher singlet Higgs masses (> 2.2 TeV), it can decay to a pair of exotic leptons, thus will produce a unique signature of two charged tracks with their invariant mass peaking at the singlet Higgs mass. This signal will be background free and probably

strengths.

¹⁰The lower limit on the mass of a heavy stable quark following the ref. [26] is 200 GeV, obtained from 8 TeV run of LHC. Due to non availability of any further updated analysis at 13 TeV, we have assumed that mass limit, on such an object, is in the ballpark of a TeV. The mass limit on heavy stable lepton [27] is 1.09 TeV. Assuming the quarks will have a higher production cross-section at the LHC, we have assumed they must be heavier than the exotic leptons.

the best bet for detection of such a scalar boson. As for example, at the 14 TeV LHC, decay of a 2.2 TeV H_S^0 will approximately produce 48 events with a pair of charged tracks with 3 ab^{-1} integrated luminosity. While we expect to have 15 such events for a 3 TeV H_S^0 at 14 TeV run with same luminosity. At 27 TeV run, the situation will improve drastically, we can expect to see 80 such events even for a 4 TeV singlet Higgs boson.

Finally we would like to make a brief comment about the situation when $c_1 + c_3 \neq 0$ and $\gamma_1 \neq 0$. Making $c_1 + c_3$ non-zero, would introduce mixing between right-handed neutral scalar with SM-like Higgs boson. However, we have to satisfy the experimentally observed signal strengths of h^0 . This in turn limits the above mixing and the H_R^0 would possibly have small decay channels to the SM fermions and SM gauge bosons. On the other hand a non-zero γ_1 would have more prominent effect on $H_R^0 - H_S^0$ phenomenology. A γ_1 induced mixing between H_R^0 and H_S^0 would lead to H_R^0 decays to SM fermions along with exotic fermions when kinematically allowed. At the same time, both these states could be produced via gluon fusion.

The production of the BSM scalars in 32121 model and the possible backgrounds have been discussed in Table 3 very briefly.

Scalars	Production at LHC	Possible final state	Possible backgrounds
$h_2^0(\xi_2^0)$	$h_2^0(\xi_2^0)b\bar{b}$	$bbbbl^+l^- \nu_l \bar{\nu}_l$	$t\bar{t}b\bar{b}, t\bar{t}h, \text{DY} + \text{jets}$
H_1^\pm	$H_1^\pm t\bar{b}$	$bbbbl^+l^- \nu_l \bar{\nu}_l$	$t\bar{t}b\bar{b}, t\bar{t}h, \text{DY} + \text{jets}$
H_L^\pm	$H_L^+ H_L^-$ pair-production	$H_L^+ H_L^-$	Stable heavy charged particle creating two charged tracks and possibly background free
—	$H_L^+ h_L^0(\xi_L^0)$	$H_L^+ h_L^0(\xi_L^0)$	Being stable and neutral $h_L^0(\xi_L^0)$ will remain undetected and H_L^+ will create one charged track and possibly background free
H_R^0	$H_R^0 A'$	$H_L^+ H_L^- l^+ l^-$	Two oppositely charged tracks of heavy stable particles, invariant mass distribution of $H_L^+ H_L^-$ should peak at $M_{H_R^0}$, background free
H_S^0	H_S^0 via gluon fusion	$E^+ E^-$	Stable heavy charged particle creating two charged tracks and possibly background free
		$qs\bar{q}s$	Stable heavy charged colored particles will hadronize

Table 3: Significant production processes of BSM scalars of 32121 at the LHC and their possible backgrounds

4 Conclusions

To summarise, we have investigated phenomenological implications of a LR symmetric model based on E_6 inspired gauge group $SU(3)_C \otimes SU(2)_L \otimes U(1)_L \otimes SU(2)_R \otimes U(1)_R$. The later symmetry group can be a result of two step breaking of E_6 . We have studied the phenomenology of the Higgs bosons, responsible for the symmetry breaking of 32121 gauge group down to the SM gauge group. The model is hallmarked by the presence of a complete family of **27**-plet of fermions belonged to the fundamental representation of E_6 . Apart from these TeV scale fermions, a weak bi-doublet (under $SU(2)_L \times SU(2)_R$), a right-handed Higgs doublet and a singlet is necessary for complete symmetry breaking. The measured value of W -boson mass fixes one of the bi-doublet vacuum expectation values, which we identify with the SM Higgs vev. The experimental lower limits on the mass of right-handed charged gauge boson W_R in turn constrain the vacuum expectation value, v_R , of the neutral member of the right-handed Higgs doublet. v_R comes out to be greater than 14 TeV. The second bi-doublet vev k_2 is set to zero to avoid a

possible admixture of W_R in the SM W boson. Appearance of an additional massive neutral gauge boson is a result of the breaking of an extra $U(1)$ symmetry. The experimental lower limit from the LHC, on the mass of such an extra $U(1)$ gauge boson puts a lower limit of 12.61 TeV on the vacuum expectation value v_S of the singlet scalar boson.

All fermions present in the 27 dimensional fundamental representation of E_6 are considered to be present in our model. We have written down the relevant dimension-4 Yukawa interactions of these fermions either with the bi-doublet scalar or the singlet scalar field, excepting the singlet lepton field L_S , for which we write a dimension-5 Yukawa term involving singlet scalar Φ_S . Furthermore, using the LHC data on the search of heavy charged long-lived particles, we have put a lower limit of 1.09 TeV on the mass of heavy exotic charged lepton.

After discussing the symmetry breaking pattern in some details, we have mainly devoted ourselves on the phenomenology of the scalars (CP-even, CP-odd and charged Higgs) present in this model. We investigated their decay modes, and possible production processes at the LHC. Without going into the details of signal background analysis we have discussed possible signatures of the Higgs bosons arising from this model.

Apart from the SM-like Higgs boson h^0 , two more neutral scalars (h_2^0 and ξ_2^0) of same mass and having similar couplings to the SM fermions will originate from the bi-doublet after SSB. Lower limit on the masses of these scalars have been obtained from the LHC data and they must be heavier than 800 GeV. Their dominant production mechanism at the LHC will be in association with a pair of b -quarks. Once produced they will mainly decay to a pair of b -quarks. The production cross-section of such scalars via gluon fusion vary from 14 (77) fb to 0.2 (1.5) fb for $m_{h_2^0} = 800$ and 1500 GeV respectively at 14 (27) TeV run of LHC.

Three more neutral Higgs bosons arise after SSB from the left and right-handed doublets. Two of them have their origin in the left-handed doublet and one in the right-handed doublet. The neutral Higgses originating from the left-handed doublet are stable and once produced in the collider they can only contribute to missing energy signature. These scalars can be good candidate for relic of the Universe. While the scalar which arise from right-handed doublet can be produced at the LHC in association with any of the neutral gauge boson (Z , Z' or A') or via vector boson fusion process. The production cross-section varies from 0.4 fb to 0.22 fb for a range of Higgs mass 400 to 1500 GeV.

Two charged Higgs bosons will be the hallmark of the model. One of them, H_1^\pm comes from the bi-doublet and this particular charged state mainly couples to a t and a b quark via Yukawa interactions. A lower limit of 720 GeV has been derived on its mass from the LHC data. The estimated cross-section for H_1^\pm production in association with tb varies from 0.15 (1) pb and 0.005 (0.06) pb for $m_{H_1^\pm} = 720$ and 1500 respectively GeV at 14 (27) TeV center of mass energy at the LHC. The rest of the charged states have origin in the left-handed doublet. They can be produced at the LHC in a mechanism similar to Drell-Yan. Once produced they will not decay. But being charged, they will leave their signature in the detector via an ionising track. In SUSY models, similar signal are produced by stable/long-lived stau. Such a signal has been looked for at the LHC by ATLAS collaboration. A lower limit on the mass of the charged Higgs H_L^\pm (> 494) GeV has been derived using the ATLAS data. We further investigate the pair-production of H_L^\pm and associated production of $H_L^\pm H_L^0$ (ξ_L^0) at LHC.

The last menu in our list is the singlet Higgs. It decays dominantly to a pair gluons and exotic fermions. We consider its production via gluon fusion at the LHC. However, production cross-section of a singlet Higgs via gluon fusion is inversely proportional to singlet vev, v_S^2 . However, v_S being in the ball park of 13 TeV, singlet Higgs production via gluon fusion fall below the level of a fb for a 1.5 TeV singlet Higgs even at 27 TeV run of the LHC.

Finally we would like to point out that, the Higgs sector of this model promises interesting phenomenology. A detail signal-background analysis has been already in our agenda [38]. Finally, the neutral $SU(2)$ singlet lepton N , Higgs bosons h_L^0 and ξ_L^0 can serve the purpose of relic. It is important to see whether they can satisfactorily fulfil the constraints from the experimental data on relic density and direct detection of dark matter [39].

Acknowledgement : SB acknowledges financial support from DST-SERB, Govt. of India in form of an INSPIRE-Senior Research Fellowship. Both the authors are grateful to Prof. Joydeep Chakraborty for introducing the subject to them and taking part in the initial stage of the work. They also thank Dr. Triparno Bandyopadhyay for several insightful discussions and comments. SB also acknowledges Dr. Tapoja Jha and Debabrata Bhowmik for useful discussions. Both of us are grateful to Prof. Amitava Raychaudhuri for several discussions on the symmetries of scalar potential.

5 Appendix:

A Masses and mixings in the particle sector of 32121 model:

Neutral CP-even scalars:

$$\begin{pmatrix} h_1^0 \\ h_2^0 \\ h_L^0 \\ h_R^0 \\ h_S^0 \end{pmatrix} = \begin{pmatrix} \cos \theta & 0 & 0 & 0 & \sin \theta \\ 0 & 1 & 0 & 0 & 0 \\ 0 & 0 & 1 & 0 & 0 \\ 0 & 0 & 0 & 1 & 0 \\ -\sin \theta & 0 & 0 & 0 & \cos \theta \end{pmatrix} \begin{pmatrix} h^0 \\ h_2^0 \\ h_L^0 \\ H_R^0 \\ H_S^0 \end{pmatrix} \quad (34)$$

where,

$$\theta = \frac{1}{2} \tan^{-1} \left(\frac{\beta_1 k_1 v_S}{\alpha_1 v_S^2 - \lambda_1 k_1^2} \right)$$

The basis on the LHS is the gauge eigenstates of the neutral CP-even scalars and the basis on the RHS shows the mass eigenstates, where θ is the mixing angle.

Charged scalars:

$$\begin{pmatrix} h_1^+ \\ h_2^+ \\ h_L^+ \\ h_R^+ \end{pmatrix} = \begin{pmatrix} c_{11} & 0 & 0 & c_{14} \\ 0 & 1 & 0 & 0 \\ 0 & 0 & 1 & 0 \\ c_{41} & 0 & 0 & c_{44} \end{pmatrix} \begin{pmatrix} H_1^+ \\ H_2^+ \\ H_L^+ \\ H_R^+ \end{pmatrix} \quad (35)$$

where,

$$c_{11} = \sqrt{1 - \frac{k_1^2}{v_R^2}} = c_{44}, c_{14} = \frac{k_1}{v_R} = -c_{41}$$

Neutral gauge sector:

$$\begin{pmatrix} W_{3L} \\ W_{3R} \\ B_L \\ B_R \end{pmatrix} = \begin{pmatrix} a_{11} & a_{12} & a_{13} & a_{14} \\ a_{21} & a_{22} & a_{23} & a_{24} \\ a_{31} & a_{32} & a_{33} & a_{34} \\ a_{41} & a_{42} & a_{43} & a_{44} \end{pmatrix} \begin{pmatrix} Z \\ Z' \\ A' \\ A \end{pmatrix} \quad (36)$$

where A is the photon and a_{ij} are the elements of the mixing matrix or the rotational matrix that rotates the gauge basis to mass basis.

$$\begin{aligned} a_{11} &= \cos \theta_W, a_{21} = \frac{-g' \sin \theta_W}{g_{2R}}, a_{31} = \frac{-g' \sin \theta_W}{g_{1L}}, a_{41} = \frac{-g' \sin \theta_W}{g_{1R}} \\ a_{14} &= \sin \theta_W, a_{24} = \sin \theta_W, a_{34} = \frac{\sqrt{\cos 2\theta_W}}{\sqrt{2}}, a_{44} = \frac{\sqrt{\cos 2\theta_W}}{\sqrt{2}} \\ a_{12} &= -1.643 \times 10^{-4}, a_{22} = 0.704, a_{32} = -0.707, a_{42} = 5.457 \times 10^{-2} \\ a_{13} &= 2.255 \times 10^{-5}, a_{23} = -0.450, a_{33} = -0.386, a_{43} = 0.804 \end{aligned}$$

B Couplings of the BSM scalars in 32121 model:

For h_2^0/ξ_2^0 :

$M_{h_2^0}$ (GeV)	$\frac{1}{\sqrt{2}}\sqrt{4\lambda_3 k_1^2 + (c_4 - c_3)v_R^2}$	$M_{\xi_2^0}$ (GeV)	$\frac{1}{\sqrt{2}}\sqrt{4\lambda_3 k_1^2 + (c_4 - c_3)v_R^2}$
$h_2^0 b\bar{b}$ coupling	$\frac{y_t}{\sqrt{2}}$	$\xi_2^0 b\bar{b}$	$\frac{y_t}{\sqrt{2}}\gamma^5$
$h_2^0 H^\pm W^\mp$	$\frac{g_{2L}}{2}\sqrt{1 - \frac{k_1^2}{v_R^2}}$	$\xi_2^0 H^\pm W^\mp$	$\frac{g_{2L}}{2}\sqrt{1 - \frac{k_1^2}{v_R^2}}$
$h_2^0 t\bar{t}$	$\frac{y_b}{\sqrt{2}}$	$\xi_2^0 t\bar{t}$	$\frac{y_b}{\sqrt{2}}\gamma^5$

For H_R^0 :

$M_{H_R^0}$ (GeV)	$\sqrt{2\rho_1 v_R^2}$
$H_R^0 h^0 h^0$	$-(c_1 + c_4)\cos^2\theta v_R - \gamma_1 \sin^2\theta v_R$
$H_R^0 H_L^\pm H_L^\mp$	$-\rho_3 v_R$
$H_R^0 h_L^0 h_L^0 / H_R^0 \xi_L^0 \xi_L^0$	$-\rho_3 v_R$
$H_R^0 h^0 H_S^0$	$(\gamma_1 - c_1 - c_4)\sin\theta \cos\theta v_R$

For H_S^0 :

$M_{H_S^0}$ (GeV)	$\sqrt{2\alpha_1 v_S^2}$
$H_S^0 ZZ$	$[\frac{g_{2L}^2 \cos^2\theta_W k_1}{2} + g_{2L}g' \sin\theta_W \cos\theta_W k_1 + \frac{g'^2 \sin^2\theta_W k_1}{2}]\sin\theta$
$H_S^0 h^0 h^0$	$-\beta_1 \sin^3\theta k_1 + 2(\beta_1 - 3\lambda_1)\sin\theta \cos^2\theta k_1$ $+2(\beta_1 - 3\alpha_1)\sin^2\theta \cos\theta v_S - \cos^3\theta \beta_1 v_S$
$H_S^0 W^\pm W^\mp$	$\frac{g_{2L}^2 \sin\theta k_1}{2}$
$H_S^0 t\bar{t}$	$\frac{y_t \sin\theta}{\sqrt{2}}$
$H_S^0 E^\pm E^\mp (H_S^0 NN)$	$\sqrt{2}y_{LB} \cos\theta$
$H_S^0 q_S \bar{q}_S$	$\frac{y_s \cos\theta}{\sqrt{2}}$

For H_1^\pm :

$M_{H_1^\pm}$ (GeV)	$\frac{1}{\sqrt{2}}\sqrt{(c_4 - c_3)(k_1^2 + v_R^2)}$
$H_1^+ t\bar{b}$	$-(y_t + y_b)\sqrt{1 - \frac{k_1^2}{v_R^2}}$
$H_1^+ h_2^0 W^- / H_1^+ \xi_2^0 W^-$	$\frac{g_{2L}}{2}\sqrt{1 - \frac{k_1^2}{v_R^2}}$

References

- [1] ATLAS collaboration, G. Aad *et al.*, *Observation of a new particle in the search for the Standard Model Higgs boson with the ATLAS detector at the LHC*, [Phys. Lett. B716 \(2012\) 1-29](#), arXiv: [1207.7214].
- [2] CMS collaboration, S. Chatrchyan *et al.*, *Observation of a New Boson at a Mass of 125 GeV with the CMS Experiment at the LHC*, [Phys. Lett. B 716 \(2012\) 30](#), arXiv: [1207.7235].
- [3] M. Mühlleitner, M. O. P. Sampaio, R. Santos and J. Wittbrodt, *Phenomenological comparison of models with extended Higgs sectors*, [JHEP08 \(2017\) 132](#), arXiv: [1703.07750]; J. Steggemann, *Extended Scalar Sectors*, [Annu. Rev. Nucl. Part. Sci. 2020. 70:197–223](#) and references therein.
- [4] C. E. Yaguna, *The singlet scalar as FIMP dark matter*, [JHEP08\(2011\)060](#), arXiv: [1105.1654]; R. Campbell, S. Godfrey, H. E. Logan and A. Poulin, *Real singlet scalar dark matter extension of the Georgi-Machacek model*, [[Phys. Rev. D 95, 016005](#)]; The GAMBIT Collaboration, *Status of the scalar singlet dark matter model*, [[Eur. Phys. J. C \(2017\) 77:568](#)]; P. Das, M. K. Das and N. Khan, *A new feasible dark matter region in the singlet scalar scotogenic model*, [[Nuclear Physics B, Vol. 964, 115307](#)];
- [5] R. N. Mohapatra and P. B. Pal, *Massive neutrinos in physics and astrophysics*, [World Sci. Lect. Notes Phys.72, 1 \(2004\)](#); N. G. Deshpande, J. F. Gunion, B. Kayser, and F. Olness, *Left-right-symmetric electroweak models with triplet Higgs field*, [Phys. Rev. D 44, 837](#); E. Ma and U. Sarkar, *Neutrino Masses and Leptogenesis with Heavy Higgs Triplets*, [Phys. Rev. Lett. 80 \(1998\) 5716-5719](#), arXiv: [hep-ph/9802445].
- [6] C. Hati, S. Patra, P. Pritimita and U. Sarkar, *Neutrino Masses and Leptogenesis in Left-Right Symmetric Models: A Review From a Model Building Perspective*, [Front. Phys., 06 March 2018](#).
- [7] A. Vicente, *Higgs Lepton Flavor Violating Decays in Two Higgs Doublet Models*, [Front. Phys., fphy.2019.00174](#); N. Ghosh and J. Lahiri, *Revisiting a generalized two-Higgs-doublet model in light of the muon anomaly and lepton flavor violating decays at the HL-LHC*, [Phys. Rev. D 103, 055009](#), arXiv: [2010.03590]; N. Ghosh and J. Lahiri, *Generalized 2HDM with wrong-sign lepton Yukawa coupling, in light of $g_\mu - 2$ and lepton flavor violation at the future LHC*, arXiv: [2103.10632]; D. Das, P. M. Ferreira, A. P. Morais, I. Padilla-Gay, R. Pasechnik and J. P. Rodrigues, *A three Higgs doublet model with symmetry-suppressed flavour changing neutral currents*, arXiv: [2106.06425]; S. Iguro, Y. Muramatsu, Y. Omura and Y. Shigekami, *Flavor physics in the multi-Higgs doublet models induced by the left-right symmetry*, [JHEP11 \(2018\) 046](#), arXiv: [1804.07478].
- [8] J. Alison *et al.*, *Higgs boson potential at colliders: status and perspectives*, [Review in Physics \(2020\) 100045](#), arXiv: [1910.00012]; G. Heinrich, *Collider Physics at the Precision Frontier*, [Physics Reports, Volume 922, 2021, Pages 1-69](#), arXiv: [2009.00516].
- [9] ATLAS and CMS Collaborations, C. Autermann, *Search for supersymmetry at the LHC*, [EPJ Web Conf. 164 \(2017\) 01028](#); A. Canepa, *Searches for supersymmetry at the Large Hadron Collider*, [Reviews in Physics 4 \(2019\) 100033](#).
- [10] J. Hewett and M. Spiropulu, *Particle Physics Probes of Extra Spacetime Dimensions*, [Annu. Rev. Nucl. Part. Sci. 2002. 52:397-424](#); T. Appelquist, H. C. Cheng and B. A. Dobrescu, *Bounds on universal extra dimensions*, [Phys. Rev. D, 64 \(2001\), Article 035002](#), arXiv: [hep-ph/0012100]; H.-C. Cheng, *Introduction to Extra Dimensions*, In: *Physics of the large and the small*, TASI 09, proceedings of the Theoretical Advanced Study Institute in Elementary Particle Physics, Boulder, Colorado, USA, 1-26 June 2009. Mar. 2011, DOI, arXiv: [1003.1162]; N. Deutschmann, T. Flacke and J. S. Kim, *Current LHC constraints on minimal universal extra dimensions*, [Physics Letters B 771 \(2017\) 515–520](#), arXiv: [1702.00410]; CMS Collaboration, *Search for resonant and nonresonant new phenomena in high-mass dilepton final states at $\sqrt{s} = 13$ TeV*, [JHEP07 \(2021\) 208](#), arXiv: [2103.02708]; CMS Collaboration, *Search for Large Extra Dimensions in the Diphoton Final State at the Large Hadron Collider*, [JHEP05 \(2011\) 085](#), arXiv: [1103.4279]; CMS Collaboration, *Search for new physics with dijet angular distributions in proton-proton collisions at $\sqrt{s} = 13$ TeV*, [JHEP 07 \(2017\) 013](#), arXiv: [1703.09986].

- [11] Y. Achiman and B. Stech, *Quark-Lepton Symmetry and mass scales in an E_6 unified gauge model*, *Physics Letters B*, **77**(4-5), 389-393; Q. Shafi, *E_6 as a unifying gauge symmetry*, *Physics Letters B*, **79**(3), 301-303; F. Gursev, P. Ramond and P. Sikivie, *A universal gauge theory model based on E_6* , *Physics Letters B*, **60**(2), 177-180; R. Barbieri, D. V. Nanopoulos and A. Masiero, *Hierarchical fermion masses in E_6* , *Physics Letters B*, **104**(3), 194-198; G. Dvali and Q. Shafi, *On proton stability and the gauge hierarchy problem*, *Physics Letters B*, **403**(1-2), 65-69.
- [12] L. Hall, Y. Nomura and D. Smith, *Gauge-Higgs unification in higher dimensions*, *Nuclear Physics B* **639**; 307–330 (2002), arXiv: [hep-ph/0107331]; Y. Abe, Y. Goto and Y. Kawamura, *Left-right symmetry, orbifold S^1/Z_2 and radiative breaking of $U(1)_R \times U(1)_{B-L}$* , *Prog Theor Exp Phys* (2018), arXiv: [1804.08836].
- [13] P. M. Ferreira, B. L. Gonçalves and F. R. Joaquim, *The hidden side of scalar-triplet models with spontaneous CP violation*, arXiv: [2109.13179].
- [14] P. S. Bhupal Dev, R. N. Mohapatra, W. Rodejohann and Xun-Jie Xu, *Vacuum structure of the left-right symmetric model*, *JHEP02* (2019) 154, arXiv: [1811.06869].
- [15] P.A. Zyla *et al.*, *Review of Particle Physics* (Particle Data Group), *Prog. Theor. Exp. Phys.* **2020**, 083C01 (2020).
- [16] T. Bandyopadhyay, G. Bhattacharyya, D. Das and A. Raychaudhuri, *A reappraisal of constraints on Z' models from unitarity and direct searches at the LHC*, *Phys. Rev. D* **98** (2018) no.3, 035027.
- [17] ATLAS Collaboration, *Search for a right-handed gauge boson decaying into a high-momentum heavy neutrino and a charged lepton in $p p$ collisions with the ATLAS detector at $\sqrt{s} = 13$ TeV*, *Phys. Lett. B* **798** (2019) 134942, arXiv: [1904.12679].
- [18] ATLAS Collaboration, *Search for new high-mass phenomena in the dilepton final state using 36.1 fb^{-1} of proton-proton collision data at $\sqrt{s} = 13$ TeV with the ATLAS*, *JHEP10* (2017) 182, arXiv: [1707.02424].
- [19] F. Staub, *SARAH 4: A tool for (not only SUSY) model builders*, *Comput. Phys. Commun.* **185**(2014) 1773, arXiv: [1309.7223].
- [20] A. Alloul, N. D. Christensen, C. Degrande, C. Duhr and B. Fuks, *FeynRules 2.0 - A complete toolbox for tree-level phenomenology*, *Comput.Phys.Commun.* **185** (2014) 2250-2300, arXiv: [1310.1921].
- [21] J. Alwall, R. Frederix, S. Frixione, V. Hirschi, F. Maltoni, O. Mattelaer *et al.*, *The automated computation of tree-level and next-to-leading order differential cross sections, and their matching to parton shower simulations*, *JHEP07* (2014) 079, arXiv: [1405.0301].
- [22] R. D. Ball *et al.*, *Parton Distributions with LHC data*, *Nucl. Phys. B* **867**, 244 (2013), arXiv: [1207.1303].
- [23] S. F. King, *Neutrino Mass Models*, *Rept.Prog.Phys.* **67** (2004) 107-158, arXiv: [hep-ph/0310204]; A. de Gouvêa, *Neutrino Mass Models*, *Annu. Rev. Nucl. Part. Sci.* **2016**. 66:197-217.
- [24] B. Stech and Z. Tavartkiladze, *Fermion Masses and Coupling Unification in E_6 . Life in the Desert*, *Phys.Rev. D* **70** (2004) 035002, [hep-ph/0311161v3]; H. Akcay, *The Fermion Masses in E_6* , *Modern Physics Letters A* **13**(09).
- [25] T. Bandyopadhyay and R. Maji, *The E_6 route to multicomponent dark matter*, arXiv: [1911.13298].
- [26] CMS Collaboration, *Searches for long-lived charged particles in pp collisions at $\sqrt{s} = 7$ and 8 TeV*, *JHEP* **07** (2013) 122, arXiv: [1305.0491].
- [27] ATLAS Collaboration, *Search for heavy charged long-lived particles in the ATLAS detector in 36.1 fb^{-1} of proton-proton collision data at $\sqrt{s} = 13$ TeV*, *Phys. Rev. D* **99** (2019) 092007, arXiv: [1902.01636].

- [28] J. Alimena *et al.*, *Searching for long-lived particles beyond the Standard Model at the Large Hadron Collider*, *J. Phys. G: Nucl. Part. Phys.* **47** 090501 (2020), arXiv: [1903.04497].
- [29] ATLAS Collaboration, *Search for heavy neutral Higgs bosons produced in association with b-quarks and decaying to b-quarks at $\sqrt{s} = 13$ TeV with the ATLAS detector*, *Phys. Rev. D* **102**, 032004 (2020), arXiv: [1907.02749].
- [30] CMS Collaboration, *Search for beyond the standard model Higgs bosons decaying into a $b\bar{b}$ pair in pp collisions at $\sqrt{s} = 13$ TeV*, *JHEP* **08** (2018) 113, arXiv: [1805.12191].
- [31] S. Dawson, C. B. Jackson, L. Reina and D. Wackerroth, *Higgs Production in Association With Bottom Quarks at Hadron Colliders*, *Mod.Phys.Lett. A* **21** (2006) 89-110, arXiv: [hep-ph/0508293].
- [32] A. V. Bednyakov, B. A. Kniehl, A. F. Pikelner and O. L. Veretin, *On the b-quark running mass in QCD and the SM*, *Nucl.Phys. B* **916** (2017) 463-483, arXiv: [1612.00660].
- [33] S. Dawson and R. Kauffman, *QCD Corrections to Higgs Boson Production: Non-leading terms in the Heavy Quark Limit*, *Phys.Rev. D* **49** (1994) 2298-2309, arXiv: [hep-ph/9310281]; D. Graudenz, M. Spira and P. M. Zerwas, *QCD Corrections to Higgs-Boson Production at Proton-Proton Colliders*, *Phys.Rev.Lett.* **70** (1993) 1372-1375.
- [34] ATLAS Collaboration, *Search for charged Higgs bosons decaying into a top quark and a bottom quark at $\sqrt{s} = 13$ TeV with the ATLAS detector*, *JHEP* **06** (2021) 145, arXiv: [2102.10076].
- [35] ATLAS Collaboration, *Search for charged Higgs bosons decaying into top and bottom quarks at $\sqrt{s} = 13$ TeV with the ATLAS detector*, *JHEP* **11** (2018) 085, arXiv: [1808.03599].
- [36] CMS Collaboration, *Search for charged Higgs bosons decaying into a top and a bottom quark in the all-jet final state of pp collisions at $\sqrt{s} = 13$ TeV*, *JHEP* **07** (2020) 126, arXiv: [2001.07763].
- [37] C. Degrande *et al.*, *Heavy charged Higgs boson production at the LHC*, *JHEP* **10** (2015) 145, arXiv: [1507.02549]; C. Degrande *et al.*, *Accurate predictions for charged Higgs production: Closing the $m_H^\pm \sim m_t$ window*, *Phys.Lett. B* **772** (2017) 87-92, arXiv: [1607.05291].
- [38] S. Bhattacharyya, work in progress.
- [39] S. Bhattacharyya, work in progress.